**Synthesis and Application of $MnO_2$/Conducting Polymer Based Multidimensional Nanocomposite for Energy Storage**

by

Xiaolong Wang

A thesis submitted to the Graduate Faculty of
Auburn University
in partial fulfillment of the
requirements for the Degree of
Master of Science

Auburn Alabama
May 4, 2013

Keywords: Manganese oxide, conducting polymer, carbon nanotube, electrochemical performance



Approved by

Xinyu Zhang, Chair, Assistant Professor of Polymer and Fiber Engineering
Sabit Adanur, Professor of Polymer and Fiber Engineering
Gisela Buschle-diller, Professor of Polymer and Fiber Engineering

## Abstract

Supercapacitors are new type of energy storage devices in addition to batteries and electrostatic capacitors. They have higher power density than batteries, and higher energy density than conventional capacitors. Moreover, supercapacitor can work under a wider range of operating temperature and longer working life. Therefore, supercapacitors have attracted a great deal of attention from the energy related society.

Currently, researches on supercapacitor mainly focus on the synthesis of high-performance electrode. The goal of this study is to establish a variety of approaches to prepare Manganese Oxide ($MnO_2$) based nanocomposites, in whichdifferent kinds of conducting materials including conducting polymer and carbon nanotube (CNT) will serve as one of the major components. Moreover, another important point of this research is to demonstrate the enhancement on capacitance of $MnO_2$ after surface modification of MnO2 by conducting materials. As for the characterizations, cyclic voltammetry (CV) and charge-discharge test are the main techniques to analyze the energy storage property. Scanning electric microscope (SEM) is used to discover the morphology of these nanocomposites and confirm the success of our synthesis methods.

This Master's thesis describes experimental details in investigating the electrochemical properties of MnO2 based nanocomposites, and confirming the potential applications as active components of supercapacitor.

Acknowledgments

The author would like to express his thanks to his advisor and mentor, Dr. Xinyu Zhang, for his time, guidance, and advice. The author also expresses his gratitude to all his committee members for their suggestions.

The author is owed special thanks to his research group partners, Yang Liu, Selcuk Poyraz and James Smith for their collaboration, guidance, and precious advice. Appreciation is also owed to another previous research group partner, Zhen Liu, for his valuable contributions during his summer internship. Thanks to the Department of Polymer and Fiber Engineering for welcoming environment.

The author finally would like to express his most sincere thanks to his parents, Yonghong Wang and Hongyan Zhu for their sincere and deeply love. The author also expresses his gratitude to all his friends in Polymer and Fiber Engineering Department and in Auburn, for providing him ongoing support throughout these two years. He also would like to express his infinite appreciation to God for bestowing him skills and ability to think.

Table of Contents

List of Tables

List of Figures

# CHAPTER 1

# LITERATURE REVIEW

## 1.1 Introduction

Since 1970s, people started to develop new electrode material for electrochemical capacitor, based on metal oxide. Companies in Russia like ESMA and ELIT had developed nickel oxide supercapacitor respectively. And the product from EMSA had been used for the power system of shuttle bus in Moscow. Moreover, America and Japan also released many types of metal-oxide based electrode materials for supercapacitor.

The earliest researches on metal oxide supercapacitor were focusing on ruthenium oxide ($RuO_2$) and iridium oxide ($IrO_2$), which are noble metal oxides [1]. $RuO_2$ can be very stable especially under aq. acidic condition, and generate relatively high specific capacitance. However, the development of these materials is pretty much limited, due to the short of noble metal resource and a high price. Instead, transition metal oxide, especially Manganese Oxide ($MnO_2$), has been found to be a good candidate with promising power and energy density for the application of supercapacitor. More importantly, environmentally friendly nature and natural abundance of MnO2 [2] will dramatically lower the cost comparing to noble metal oxide.

Figure 1 Manganese oxide powder

However, the drawback of $MnO_2$ is its relatively low electric conductivity, which will severely limit its performance as capacitor [2]. But more and more attempts have been brought out to solve this problem. A typical approach is to composite $MnO_2$ with conducting materials such as conducting polymers or carbon nanotubes.

### 1.2 Manganese oxide, $MnO_2$

Manganese (IV) oxide is an inorganic compound with chemical formula $MnO_2$. [3] This black or brown solid present naturally as the mineral pyrolusite, which is the major mine of manganese and a component of manganese compounds. Basically the utility for $MnO_2$ is for batteries, such as the alkaline battery and the zinc-carbon battery. [4] Moreover, $MnO_2$ is also a precursor to produce other manganese compounds, such as $KMnO_4$ or $MnSO_4$.

Natural manganese oxide is always with impurities and a considerable scale of manganese in its 3+ valence state. [3] Only a limited number of manganese mine contain high composition γ–$MnO_2$, which is normally used for battery industry. Thus the production of synthetic manganese oxide is important. There are totally two kinds of methods are used, producing chemical manganese oxide (CMD) and electrolytic manganese oxide (EMD). The CMD is mostly used for the production of ferrites, while EMD is used for the production of batteries. [5]

Manganese element has many different complex oxides system such as $MnO_2$, $Mn_2O_3$ and $Mn_2O_7$. The reason is that a variety of possible oxidation states of Mn (+3, +4, +5 and +7) presenting in nature. Manganese oxide materials are very important in technological applications including supercapacitor, catalysts, ion sieves, and cathodic materials in lithium batteries because of outstanding structural flexibility plus novel

physical and chemical properties. [6-7] Among the serials of manganese oxides, $MnO_2$ exhibits the largest number of polymorph structures. Not less than fourteen modifications have been mentioned in literature. [8] The reason for it could be the small ionic radius of $Mn^{4+}$ (R = 0.53 Å). Even though such a small ionic radius could result in a tetrahedral coordination, the $3d^3$ electronic configuration of $Mn^{4+}$ stabilizes octahedral coordination which accounts for the absence of tetrahedral coordinated $Mn^{4+}$ in oxides [9-11]. All of the $MnO_2$ structures can be summarized as a distribution of $Mn^{4+}$ in the interstices of several close-packed networks of oxygen atoms. [12] The complexity is the result from a fact that different kinds of cation ordering schemes are possible in $MnO_2$.

### 1.3 Conducting polymers

Conducing polymer is another major component in the nanocomposite, which could possibly help to enhance the electrical conductivity. In 1958 Natta et al. [13] succeeded in synthesis of polyacetylene, a black powder, as the first prototype of conducting polymer. Polyacetylene exhibits electrical conductivity due to the presence of extended π-bond conjugation, which allows charge carrying along on the polymer backbone[13] with values between $7x10^{-11}$ to $7x10^{-3}$ S/cm [14](semi-conductor level). The conductivity range of the as-produced conducting polymer is mainly depending on how it was synthesized. Conducting polymer research made its major breakthrough [13] in late 70's after a collaboration of scientists Hideki Shirakawa, Alan G. MacDiarmid and Alan J. Heeger [13]. At that time, chemists Shirakawa and MacDiarmid were focused on the research about the conductivity improvement of polyacetylene according to a doping process, which was also adopted by physicist Alan J. Heeger. The conducting polymer used in our research is polypyrrole. Polypyrrole is one of the most widely researched chemical among intrinsic conducting polymer family, in different areas of science and industry. The first information

about the conductivity level of iodine doped, chemically oxidized polypyrrole can be dating back to 1963 [15].

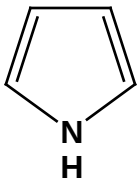


Figure 2 Chemical structure of pyrrole monomer

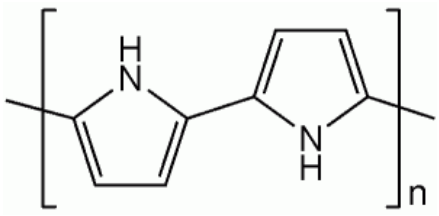


Figure 3 Chemical structure of polypyrrole

The picture above show the chemical structure of pyrrole and polypyrrole, which is a conjugated material allowing the electrons being transferred along the polymer chains. Polypyrrole can be considered as the first derivative of polyacetylene that exhibits a high level of conductivity. Researches on polypyrrole have been extended to very broad areas in chemistry and polymer science, in order to establish a solid knowledge base and to improve the properties of this polymer for further applications.

### 1.4 Typical researches on $MnO_2$/conducting materials based supercapacitor

There are many efforts made to enhance the capacitance of $MnO_2$ based composite, especially with conducting materials like conducting polymer. Dr. Xiaodong Li et al. [16] have reported a remarkable research on the enhancement of $MnO_2$ capacitance by composited it with polypyrrole. The specific capacitance of $MnO_2$ powder can reach 294 F/g if the size of $MnO_2$ decreases to a nanoscale. They reported an approach to synthesize

ultrafine $MnO_2$/polypyrrole nanorod composite powders at room temperature. [16] In this synthesis method, pyrrole monomer is a reductant to reduce $Mn^{7+}$ ions in $KMnO_4$ solution to $Mn^{4+}$ ions in the form of $MnO_2$ crystal. At the same time, the pyrrole monomers go through an oxidative polymerization process to form conductive polypyrrole. [16]

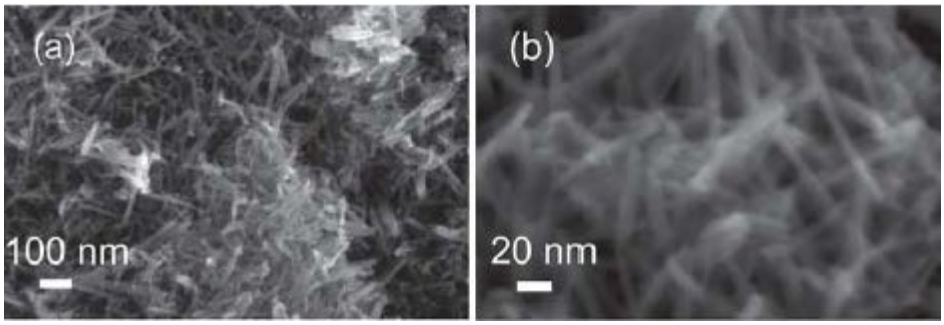


Fig 4 SEM images of $MnO_2$/polypyrrole nanorod composite [16]

In Figure 4, the rod like $MnO_2$ is entangled with granular PPy to form nanocomposite. The $MnO_2$/PPy nanocomposite powders were further used to prepare supercapacitor electrodes, which were then characterized by cyclic voltammograms (CV). The CV curve of the as-prepared supercapacitor, at different scan rates in 1 M $Na_2SO_4$, is shown in figure 5.

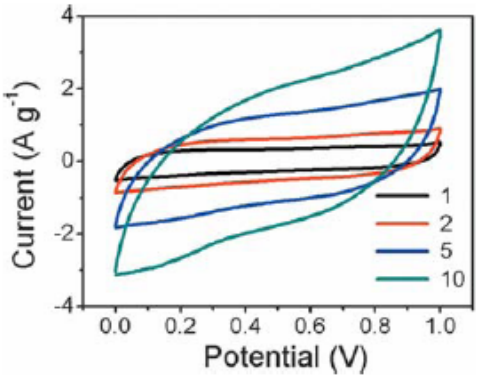


Fig. 5 CV curve of the MnO2/PPy nanorod composite electrode at different scan rate [16]

The rectangular shape of the CV curves indicates a typical capacitor characteristic, which will be explained in detail in characterization part (chapter 3).

Dr. Jaidev et al. [17] report a facile approach for synthesis of a novel Polyaniline (PANI)/$MnO_2$ nanotube (MNT) hybrid nanocomposite by in situ polymerization. This nanocomposite combines the advantages of $MnO_2$, low cost and high power density, with the PANI's high electrical conductivity. Here is SEM image of as-produced samples shown as Figure.6 in which the $MnO_2$ tubes go through into a bulky PANI granule.

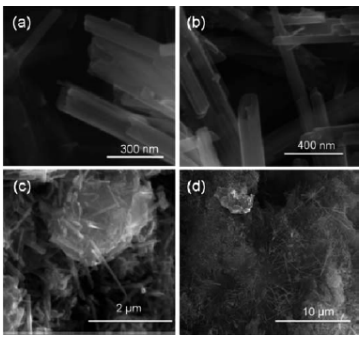


Fig. 6 SEM images of as prepared MNT (a and b), and PANI/MNT hybrid (c and d). [17]

In the electrochemical application, a CV test has been made. As a result, a rectangular shape can promise its stable nature to serve as supercapacitor. Here is the CV test at different scan rate in Figure 7.

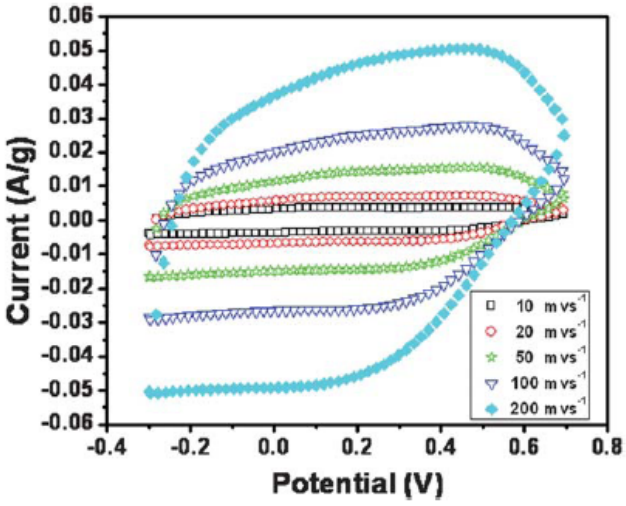


Fig 7 Cyclic voltammograms of PANI/MNT hybrid at various scan rates. [17]

To calculate the specific value of capacitance, the researchers also use charge-discharge test as a general method. Here is the result for this test.

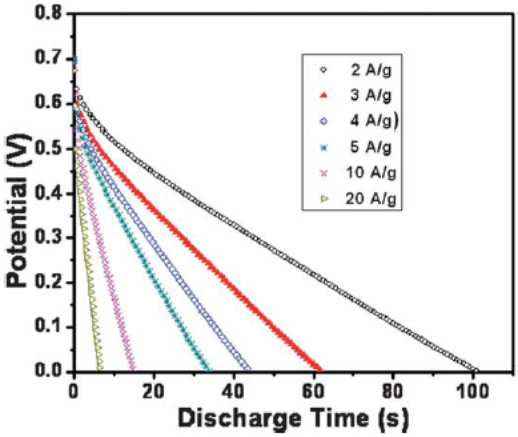


Fig 8 Discharge curve of PANI/MNT hybrid at different specific current densities. [17]

The hybrid nanocomposite shows a high capacitance value of 626 F/g [17] after calculation by the general equation, which will be explained in detail at the characterization part. The synthesis method they reported can be further extended to prepare other hybrid structures of metal oxide nanotubes and conductive polymers, such as polypyrrole, the conducting polymer adopted in our research.

### 1.5 **Microwave Initiated Carbonization of Nanocomposite Samples**

There have been lots of researches claimed that microwave can initiate the carbonization of conducting polymer in a very short time and generate tremendous amount of heat [18] With addition of proper precursor, one can expect microwave can assist carbon nanotube growth. [26] Please note that the sample has to be conductive or at least with a conductive layer of coating, can the samples be heated under the microwave irradiation. The interactions between microwave irradiation and different types of materials shall be made sure carefully. And the key property of the heating materials is the conducting nature.

Researches have shown that materials within a moderate conductivity (intrinsically conducting polymers) levels from $10^{-5}$ to 10S/cm can be heated more efficiently than insulating or highly conductive materials. [19, 25] Moreover, only conducting materials are not enough to produce carbon nanotube (CNT) with microwave due to the lack of carbon precursor. One of the most reliable carbon precursors is ferrocene, which has been widely used to produce carbon based composite. Here is the chemical structure of ferrocene,

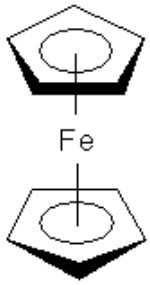


Figure 9 Chemical structure of ferrocene [20]

The ratio of carbon in ferrocene is high enough to provide the source of carbon. In terms of the iron atom in the structure, it can serve as the catalyst to initiate the growth of CNT on the surface or among the conducting substrate.

Another important property that impacts the performance of the microwave treatment is the dimensions of the material. Smaller conductor has better efficiency in absorbing the microwave irradiation [25]. Nanostructured conducting polymers with moderate conductivity could absorb microwave energy in a very efficient way, which makes them promising candidates of the rapid heating process [18]. Since huge amount of heat can be generated by microwave irradiation on the conducting polymers, the precursor ferrocene will then be quickly converted to CNT. In this work, due to the low conductivity nature of $MnO_2$, a conducting coating, polypyrrole, is needed in order to ensure the quick heating of the

system for the growth of CNT. Figure 10 showed the reagent and product in a typical microwave process.


Figure 10 Microwave initiated carbonization to produce CNT based nanocomposites

Since a high temperature will lead to inflation of air inside the glass vial, which is used to contain PPy/ferrocene blend, care should be taken in case of explosion of glass vials due to the rapid increase of temperature and pressure inside during the small-scale productions. Finally, samples with nanoscaled morphology were collected and stored carefully for further characterization. To test the morphology and other property changes, after microwave treatment, of selected nanocomposite samples, various characterization tests were applied and the obtained results were discussed in the following chapter of this master's thesis.

# Chapter 2

## Synthesis of Manganese oxide/Polypyrrole/CNT nanocomposite

### 2.1 Experimental section

#### 2.1.1 Materials

*For the synthesis of Commercial $MnO_2$ based nanocomposite*

Manganese oxide (98%), pyrrole (98+%), ammonium peroxydisulfate (APS $(NH_4)_2S_2O_8$) 98%, ferrocene (99%) and hydrate chloride (HCl) to prepare diluted HCl were all purchased from Alfa Aesar and used as received.

*For the synthesis of solid-phase $MnO_2$ (Manganese Nitrate as the precursor) based nanocomposite*

Manganese nitrate ($Mn(NO_3)_2$), ferrocene (99%) and were purchased from Alfa Aesar and used as received. PPy nanofiber was synthesized in advance.

*For the synthesis of Microwaved MnO2 (Manganese Nitrate as the precursor) based nanocomposite*

Manganese nitrate ($Mn(NO_3)_2$), pyrrole (98+%), ammonium peroxydisulfate (APS $(NH_4)_2S_2O_8$) 98%, ferrocene (99%) and hydrate chloride (HCl) to prepare diluted HCl were all purchased from Alfa Aesar and used as received.

#### 2.1.2 Synthesis Methods

##### 2.1.2.1 Synthesis of Commercial $MnO_2$ based nanocomposite

As mentioned at the very beginning, $MnO_2$ can be composited with a variety of conducting materials with different kinds of methods. Firstly, to composite $MnO_2$ with PPy, we use aqueous-phase method to synthesis the $MnO_2$/PPy hybrid in the solution of HCl. Then this hybrid would be blended with ferrocene which is the precursor of CNT by using a speed mixer for 3 minutes at a mixing speed of 3500rpm. Finally, we use microwave to

heat the blend, continue to heat it for 2 minutes until no burning in glass vial to get the MnO2/CNT two-component nanocomposite. The morphology of the sample under the SEM characterization is the first concern. In other words, there could be a considerable amount of CNTs in the sample Thus; we have several control experiments to synthesis MnO2/PPy hybrid in order to get the optimism ratio between each reagent, which will finally determine the morphology of MnO2/CNT nanocomposite. Here are the tables listing all of the control experiments we have done for this project.

| NO. | MnO2 | Pyrrole (Py) | HCl (50mL) | APS (oxidant) | Ratio of MnO2 to Py |
|---|---|---|---|---|---|
| 1 | 1g | 1mL | 1M | 1.15g | 1:1 |
| 2 | 1g | 0.5mL | 1M | 0.6g | 2:1 |
| 3 | 2g | 0.5mL | 1M | 0.6g | 4:1 |
| 4 | 3g | 0.5mL | 1M | 0.6g | 6:1 |

Table 1 Summary of controlled condition (Ratio of $MnO_2$ to Pyrrole)

The optimized condition has been determined by comparing the morphology of final sample ($MnO_2$/CNT) produced from these 4 groups of $MnO_2$/PPy hybrid. The ratio of 4:1 is the optimized condition. (The morphology for the nanocpmposites will be presented in chapter 3)

| NO. | MnO2 | Pyrrole | HCl (50mL) | APS | Ratio MnO2 : Py |
|---|---|---|---|---|---|
| 5 | 2g | 0.5mL | 0.1M | 0.6g | 4:1 |
| 6 | 2g | 0.5mL | 0.2M | 0.6g | 4:1 |
| 7 | 2g | 0.5mL | 0.5M | 0.6g | 4:1 |
| 8 | 2g | 0.5mL | 1.0M | 0.6g | 4:1 |

Table 2 Summary of controlled condition (concentration of HCl)

After determining the ratio of MnO2 and pyrrole, the concentration of HCl was taken as another factor to impact the morphology of final product. Still we judge the optimized condition by comparing the morphology of final sample and then 0.5M as the concentration of HCl is determined as the optimized condition.

For the detail, in a typical synthesis of PPy/MnO2 hybrid, 2g MnO2 is firstly dispersed in 50mL of 0.5M aqueous HCl. After magnetic stirring for 5 min, 0.5mL pyrrole is added and stirring is continued for an additional 10 min. Finally, 0.6g Ammonium Persulfate (APS) is added to start the polymerization. After 3 hours, a black precipitate of MnO2/PPy hybrid is suction-filtered and then washed with 1M HCl, drying in an oven ($80^{o}$C) for 2 hours.

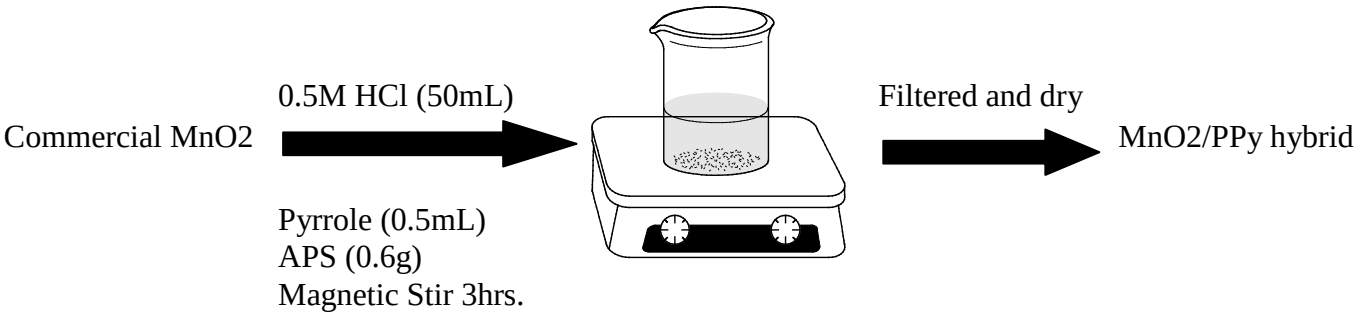


Figure 11 Synthesis of as-purchased MnO2/PPy hybrid

As for the coming microwaving step, weighing 70mg of the as-synthesized hybrid and we blend it with ferrocene by a mass ratio of 1 to 1. Setting the parameter of mixer with a speed of 3500rpm and blending for 3 minute. After the step of mixing, we transfer the blend into a glass vial and put it into the microwave, heating the sample until burning can be seen inside the vial. Then heating is continued for another 2 minute until fire can not be seen. Cooling the sample in nature and then put it into an oven under the temperature of 80 $^{o}$C in order to remove the ferrocene residue.

Figure 12 Sample burning in microwave

Figure 12 is a typical microwave process. Blend (mainly the conducting polymer) will absorb the energy from microwaving irradiation and start to burn, leading to the intense conversion from the source of carbon to carbon nanotube.

### 2.1.2.2 Synthesis of Microwaved $MnO_2$ based nanocomposite

In this project, we firstly use manganese nitrate as the precursor to produce MnO2 instead of immediately using purchased MnO2. Then the as-produced MnO2 will follow the same procedure to synthesis MnO2 based composite. Here the "microwaved" means synthesize MnO2 from manganese nitrite by a microwaving process.

Manganese (II) nitrate is an inorganic compound with formula $Mn(NO_3)_2$. Each formula unit is composed of one $Mn^{2+}$ cation and two $NO_3^-$ anions and varying amounts of water. Most common is the tetrahydrate $Mn(NO_3)_2 \cdot 4H_2O$, but mono- and hexahydrates are also known as well as the anhydrous compound. The chemical compound is useful precursors to the oxides of manganese in industry because of its natural abundance, lower cost comparing to MnO2 and a mature way to produce the oxides of manganese in industry. The price of manganese nitrate has been checked from several chemical selling companies such as Alfa Aesar, $Mn(NO_3)_2$ 98% as an example, which only costs 32 U.S. dollars per 25 gram. In comparison, 5 gram of 98% meshed MnO2 will cost 32 dollars, which means that the price of MnO2 is 5 times than $Mn(NO_3)_2$. Moreover, to produce MnO2 from manganese nitrate is pretty straightforward in industry because $Mn(NO_3)_2$ will decompose under the temperature around 400$^o$C. At temperatures of 400 °C, the salt decomposes, releasing $N_2O_4$ and leaving a residue of purified manganese oxide.

$$Mn(NO_3)_2 \xrightarrow{\text{Microwave}} MnO_2 + N_2O_4$$

Figure 13 Chemical formula of $Mn(NO_3)_2$ decompose reaction

This reaction conduction is very easy to be achieved by using a microwave because the decomposed temperature can be easily reached under a microwave irradiation. So we can use microwave as a small-scale industrial production.

Figure 14A $Mn(NO_3)_2$ before microwave

Figure 14B $Mn(NO_3)_2$ during microwave

Figure 14C $Mn(NO_3)_2$ after microwave

In Figure 14, we can find that after microwaving, the white salt crystal is converted into black powder which will be proved as $MnO_2$ in the characterization part. And during the microwave, a large amount of brown $N_2O_4$ will be released, indicating that the reaction can be processed in the condition of microwave irradiation. In a typical production of $MnO_2$, weighing 10mg of $Mn(NO_3)_2$ crystal and putting it into a glass vial. Setting the microwave at the highest level and heating the sample. Please note that a large amount of harmful gas will be released. So this reaction needs to be processed in a hoop. And the researchers need to wear a mask. Moreover, since the reaction is very intense, we need to stop the microwave for about 5 seconds every 10 seconds in order to avoid explosion of glass vial. After heating, cooling the black powder in nature and preparing for the next step.

After obtaining the pure as-produced MnO2, we just follow the procedure that synthesizing the purchased meshed MnO2 based nanocomposite because the optimal ratio of each reagent has been determined. We adopt this optimal reacting condition into this project.

In a typical synthesis of PPy/MnO2 hybrid, 2g MnO2 is firstly dispersed in 50mL of 0.5M aqueous HCl. After magnetic stirring for 5 min, 0.5mL pyrrole is added and stirring is continued for an additional 10 min. Finally, 0.6g Ammonium Persulfate (APS) is added to start the polymerization. After 3 hours, a black precipitate of MnO2/PPy hybrid is suction-filtered and then washed with 1M HCl, drying in an oven (80$^{o}$C) for 2 hours.

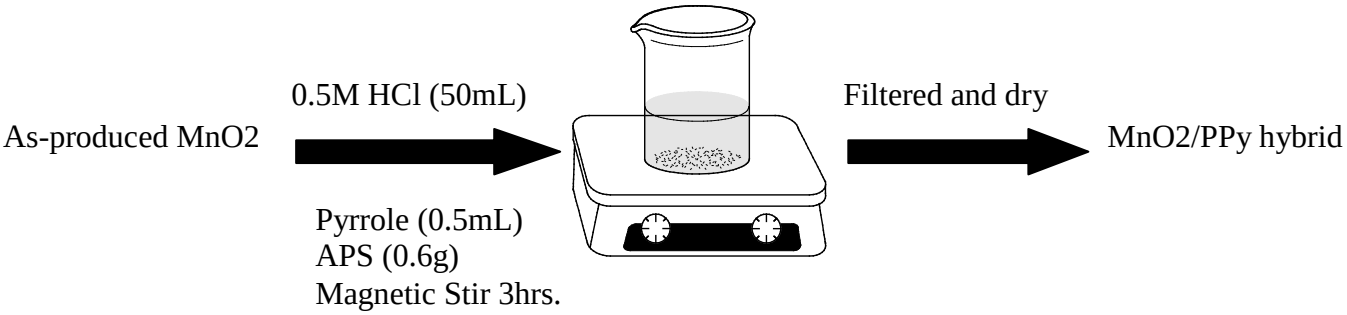


Figure 15 Synthesis of as-produced MnO2/PPy hybrid

The as-synthesis hybrid also has a potential that growing CNT in the condition of microwave heating. As for the coming microwaving step, weighing 70mg of the as-synthesized hybrid and we blend it with ferrocene by a mass ratio of 1 to 1. Setting the parameter of mixer with a speed of 3500rpm and blending for 3 minute. After the step of mixing, we transfer the blend into a glass vial and put it into the microwave, heating the sample until fire can be caught inside the vial. Then heating is continued for another 2 minute until fire can not be seen. Note that since the reaction is very intense, in case of the explosion of glass vial, we need to stop microwave every 10 to 15 seconds and shake the glass vial to allow the sample being burned uniformly. Finally, cooling the sample in nature and then put it into an oven under the temperature of 80 $^{o}$C for 24 hours in order to remove the ferrocene residue.

#### 2.1.2.3 Synthesis of solid-phase $MnO_2$ based nanocomposite

To the best of our knowledge, even though $MnO_2$ doesn't react with diluted acid such as 0.5M HCl,, still there are some loss for $MnO_2$ during the aqueous-phase reaction where diluted HCl as the solvent. A part of MnO2 will be solved into manganese cation $Mn^{2+}$. In the last two sections of experiments, we both synthesize MnO2/PPy hybrid in an aqueous phase with an acidic condition. So the loss of stuff is inevitable. In order to not only avoid the wastage but also ensure the stuff can be composited with PPy, here we come up with a new idea that immediately physically blend Mn(NO3)2 with as-synthesized polypyrrole nanofiber and then microwave the blend to obtain the MnO2/PPy hybrid. In this method, we can waive the aqueous-phase reaction and still obtain the composite. Here what we induced is PPy nanofiber. The reason to use nanostructure but not the common granule is that much larger surface area can be given by a nanostructure comparing to a bulk one, allowing more amount of MnO2 particle attached on the surface of PPy. Moreover, the nano conducting polymer has a better electrochemical property.

For the purpose to get the optimal ratio of Mn(NO3)2 and PPy nanofiber, we have several control experiments and test the morphology of hybrid by SEM. The standard to judge the morphology is that MnO2 particles disperse among the PPy nanofiber uniformly.

We control the mass ratio of Mn(NO3)2 and PPy nanofiber by 1 to 1, 2 to 1 and 3 to 1 respectively. As a result, the ratio of 2 to 1 gets the best morphology under the SEM test (mentioned in detail at Chapter 3). In a typical production of solid-phase MnO2/PPy hybrid, weighing manganese nitrate and PPy nanofiber as a mass ratio of 2 to 1 and blend them in a speed mixer. Setting the parameter of mixer with a speed of 3500rpm and blending for 3 minute. Then transfer the blend into a glass vial and put it into the microwave, heating the sample until there is no brown gas (N2O4) released from the vial. Cooling the sample in nature and prepare for next step.

In this project, there are totally 2 steps. And both of these steps are microwave processing. In the next step, weight 70mg of as-produced MnO2/PPyNf hybrid mixing with the same amount of ferrocene. Then follow the same microwave procedure mentioned in the last experimental section to obtain the MnO2/CNT nanocomposite.

#### 2.1.2.4 Purification of As-prepared Samples

In the part of synthesis 1 and 2, we both use aqueous phase as the reaction medium. So there could be a variety of impurities left after the reaction. So a post-purification is needed to ensure the sample is available for the next step.

At the end of the specific polymerization times (3hours for PPy polymerization with MnO2) all different types of reaction solutions containing the black precipitates of polymeric structures were gone through the same purification process. Each and every prepared sample was washed and suction filtered, in a Whatman 70mm diameter filter paper equipped[21] Buchner funnel, which was attached to a water respirator, by using copious amounts of DI water (3x100mL) -to remove the residual monomers and its water soluble decomposition by products with the oxidant- and Acetone (3x100mL) -to remove low molecular weight organic intermediates and oligomers [21] from the system and to facilitate the drying process of the as-prepared samples with the quick evaporation of acetone. The wet dark blue or dark brown precipitates were allowed air drying (5-10min.) inside the funnel until there was no more liquid left to suck from the filter paper.

### 2.1.3 Preparation of Electrodes for the Cyclic Voltammetry (CV) Applications

For the CV test, graphite rods and colloidal graphite were utilized to prepare electrodes for the supercapacitor applications. Graphite rods were modified to decrease the amount of surface and material amount interacting with the alligator clips and the electrolyte solutions. At the effective tips of the graphite rods (working electrode) which were placed into the electrolyte, colloidal graphite was applied to be able to paste as-prepared samples. A

clean platinum wire is used as counter electrode. Ag/AgCl in a saturated solution of potassium chloride KCl is used as the reference electrode.

### 2.1.4 Instruments and Characterization Methods

*Thermogravimetric Analysis (TGA);* a TA Instruments TGA Q500 thermogravimetric analyzer was used to characterize the thermal properties of PPy/MnO2 structures with different morphologies and synthesis methods. ~5mg to 10mg of each sample was exposed to thermal heating under pressurized air, from room temperature to 900°C at 10°C/min rate.

*Scanning Electron Microscopy (SEM);* a Zeiss EVO 50 variable pressure scanning electron microscope with digital imaging and EDS, was used to characterize the morphological properties of very small pieces of above mentioned samples. An EMS 550X auto sputter coating device with carbon coating attachment was also utilized for gold sputtering of samples, which were readily prepared on carbon tape mounted sample holders, before testing them at SEM.

*Electrochemical Cyclic Voltammetry (CV);* voltammetric data of three groups of different samples (Purchased MnO2 serials, aqueous-phase serials and solid-phase serials) were recorded at standard laboratory conditions by an Arbin electrochemical instrument (Arbin-010 MITS Pro 4-BT 2000). Tests were conducted by applying 0V to 1.0V at a scan rate of 20mV/s to the so-called samples--coated electrodes in KCl electrolyte, according to the way described earlier.

*Fourier Transform Infrared (FT-IR) Spectroscopy;* all the IR Transmittance spectra were recorded by a Thermo Fischer Scientific NICOLET 6700 FT-IR instrument. This device uses an attenuated total reflectance (ATR) module that collects IR spectra independently from sample size and without any further sample preparation requirement for solid and liquid samples, between wave number ranges of $500cm^{-1}$ to $2000cm^{-1}$.

*Elemental Analysis;* weight %s of O, Mn elements within each as-prepared nanocomposite were measured by Oxford Instruments, INCA EDX instrument to verify and determine the exact chemical formulas of the sample products obtained.

# CHAPTER 3

# RESULTS AND DISCUSSIONS

All different samples obtained through these experiments were characterized through different perspectives by using various characterization techniques to build a substantial knowledge for the promising future applications of these structures. Characterization results collected during the tests and applications mentioned at the previous chapter of so-called MnO2 based nanocomposite structures were discussed in a detailed and comprehensive manner along the following sections of this chapter. In this chapter, I will explain the characterization results respectively of the samples obtained by the 3 experimental methods mentioned in chapter 2.

## 3.1 Characterizations for Commercial $MnO_2$ based nanocomposite

### 3.1.1 SEM Characterization Results

Different morphology of manganese oxide structures were initially characterized by SEM to verify and prove the success of above mentioned synthesis methods.

Since we purchased the as-produced meshed MnO2 from chemical company, it is necessary to firstly test the morphology of this raw material as the control sample.

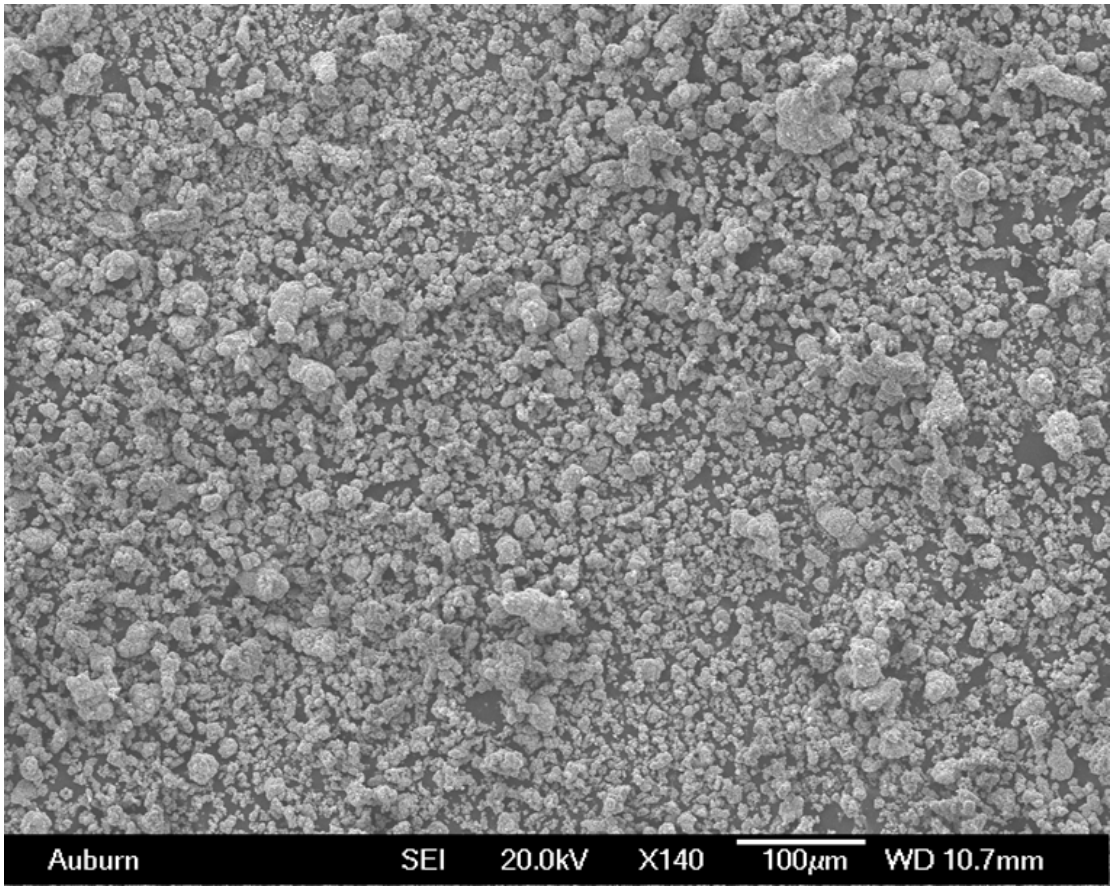


Figure 16 SEM image of purchased pure $MnO_2$ mesh

The SEM image above showed the amorphous microstructure of the pure MnO2. There is no nanostructure but granule. So the possibility that pure MnO2 make a contribution to nanostructure can be ruled out.

There are totally 7 groups of controlled experiments to synthesize MnO2/PPy hybrid as mentioned in chapter 2. The ratio of MnO2/Pyrrole and the concentration of HCl are the controlled factors. The standard to justify the optimal condition is the morphology of MnO2/CNT nanocomposite obtained after microwaving the blend of MnO2/PPy hybrid and ferrocene. Below are the SEM images of MnO2/CNT (microwaved MnO2/PPy with ferrocene) samples from those 7 groups of controlled methods.

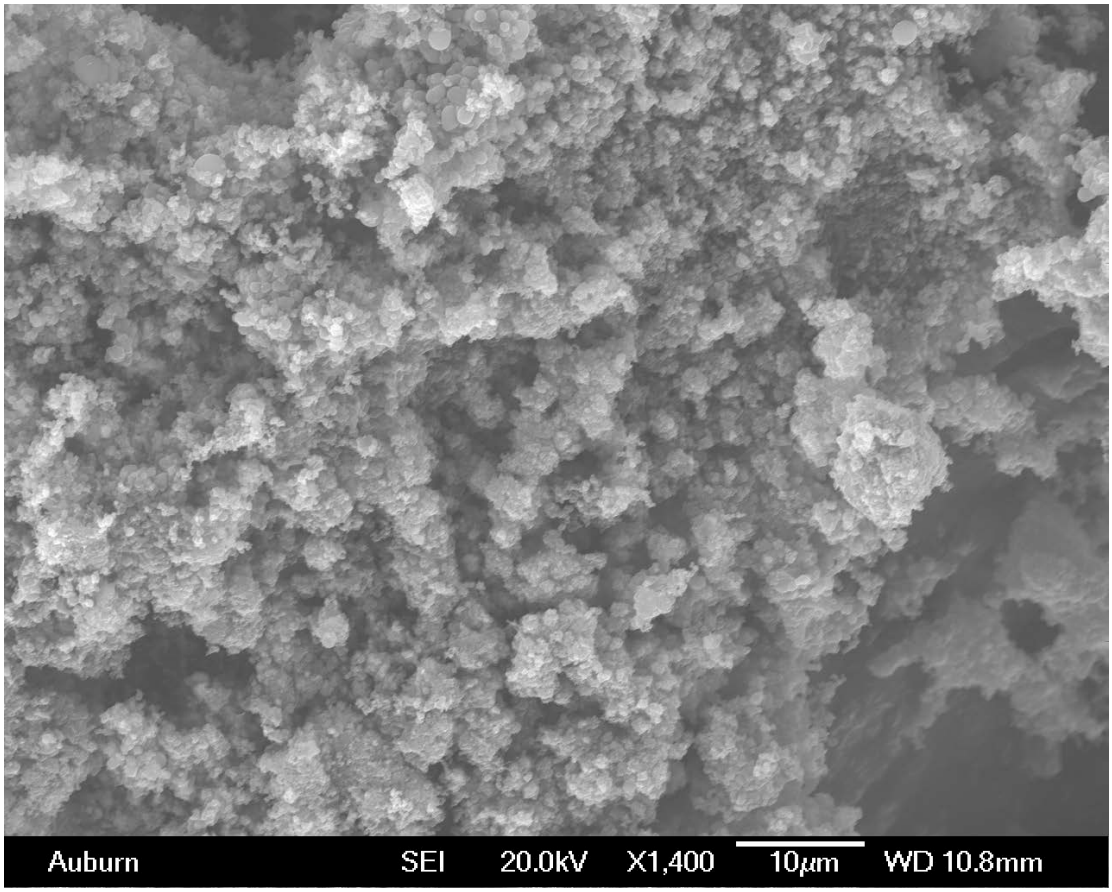


Figure 17 SEM images of MnO2/CNT sample the ratio of MnO2 and Py is 1:1 in 1MHCl

The SEM image above showed that there is basically no CNT obtained following the ratio of 1 to 1 after microwave. By increasing the ratio of MnO2 to 2:1, It can be find in the SEM image that there are a few of CNT growing after microwave. Here is the SEM picture.

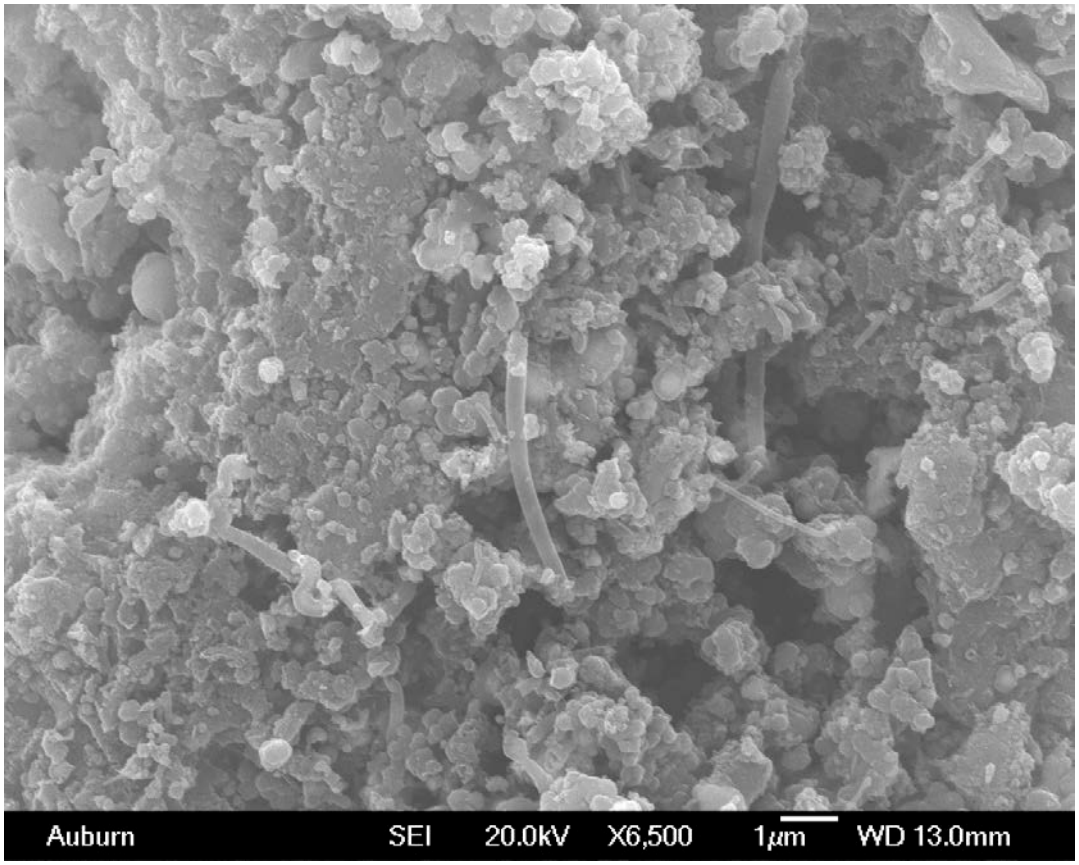


Figure 18 SEM images of MnO2/CNT sample the ratio of MnO2 and Py is 2:1 in 1MHCl

In SEM image shown above, a small amount of tube-like structure with a diameter of around 500nm can be found which is not the typical CNT because of the over large diameter (the common diameter of carbon nanotube is below 100nm). By increasing the ratio of $MnO_2$, the amount of CNT can also be increased. Thus, we further increase the ratio of $MnO_2$/Py to 4:1 in order to obtain larger amount of and much thinner CNT.

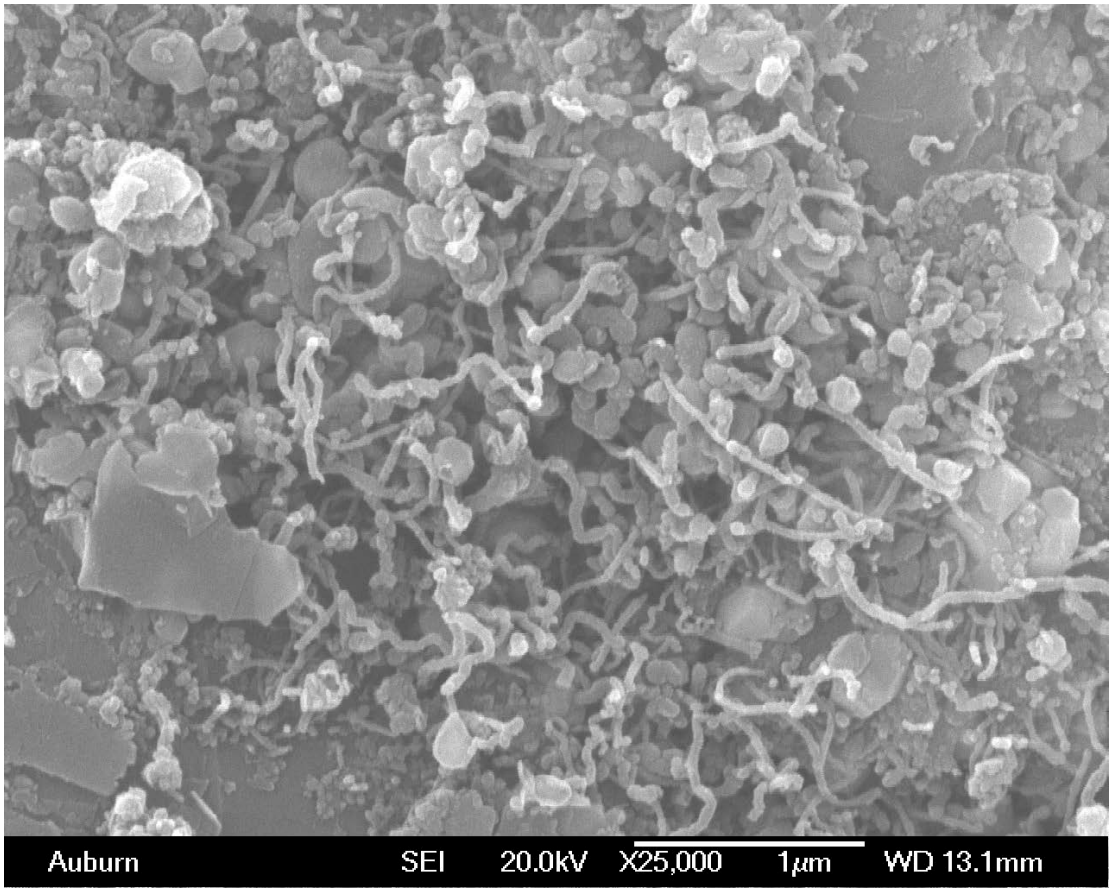


Figure 19 SEM images of MnO2/CNT sample the ratio of MnO2 and Py is 4:1 in 1MHCl

Much more CNT can successfully grow by following the ratio of 4:1. Moreover, the diameter of CNT is just around 10nm within a standard range. We can also find the granule MnO2 among CNT. So the MnO2/CNT nanocomposite can be successfully produced by microwaving method. In order to test whether the ratio of 4:1 is the optimal one, we further increase the ratio to 6:1 to observe the difference.

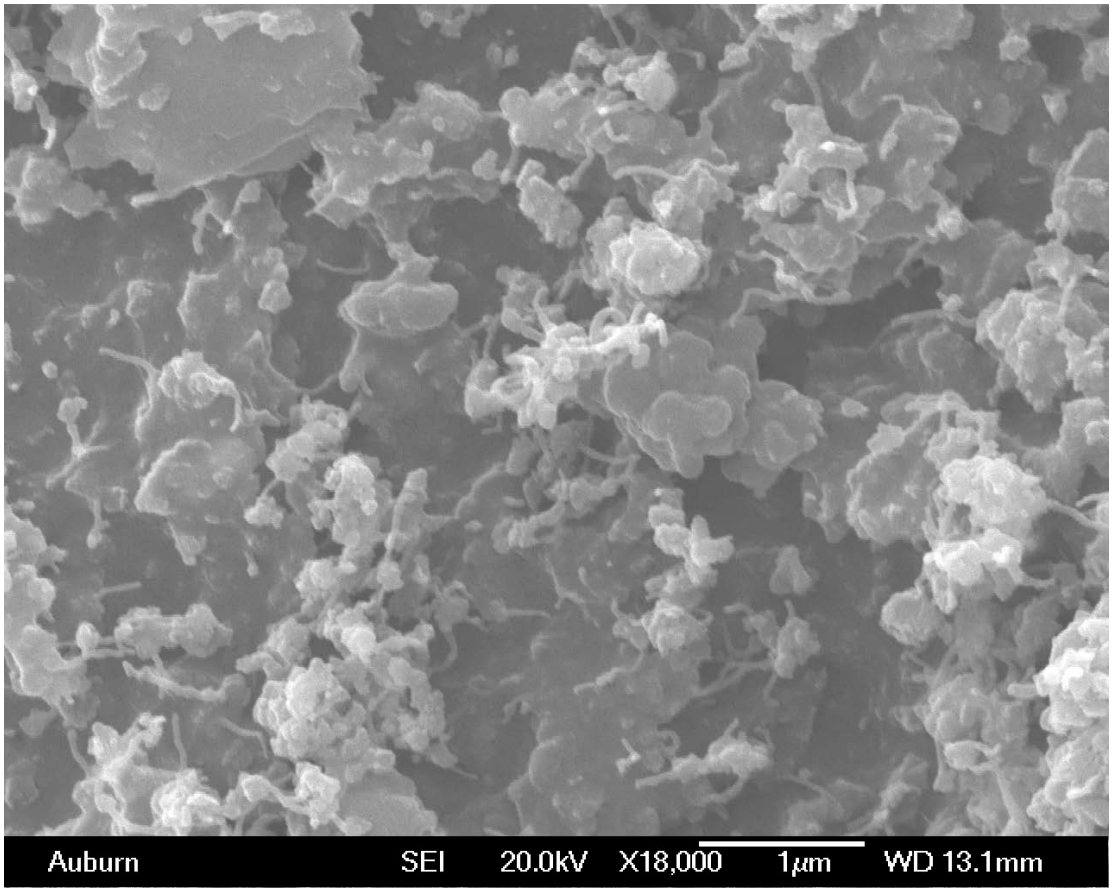


Figure 20 SEM images of MnO2/CNT sample the ratio of MnO2 and Py is 6:1 in 1MHCl

Comparing to the ratio of 4:1, the amount of CNT decreased. So the relation between the MnO2/Py ratio and the final amount of CNT is like a conic curve in which 4:1 is at the maximum amount. So by following these serials of controlled experiments, we determined the optimal ratio of MnO2 and pyrrole. In the next step, the concentration of hydrochloric acid (HCl) is another controlled factor.

It has been considered that different concentrations of HCl may affect the final structure of MnO2/CNT because HCl serve as not only the solvent but also the doped agent for PPy. A higher concentration of HCl can lead to the better conductivity of PPy. Further, better conductivity can result in a better burning condition during the microwave and thus more amount of CNT can be produced. In these serials of controlled experiments, we

have a certain ratio of MnO2/Py 4:1 which has been determined above with a changing HCl concentration.

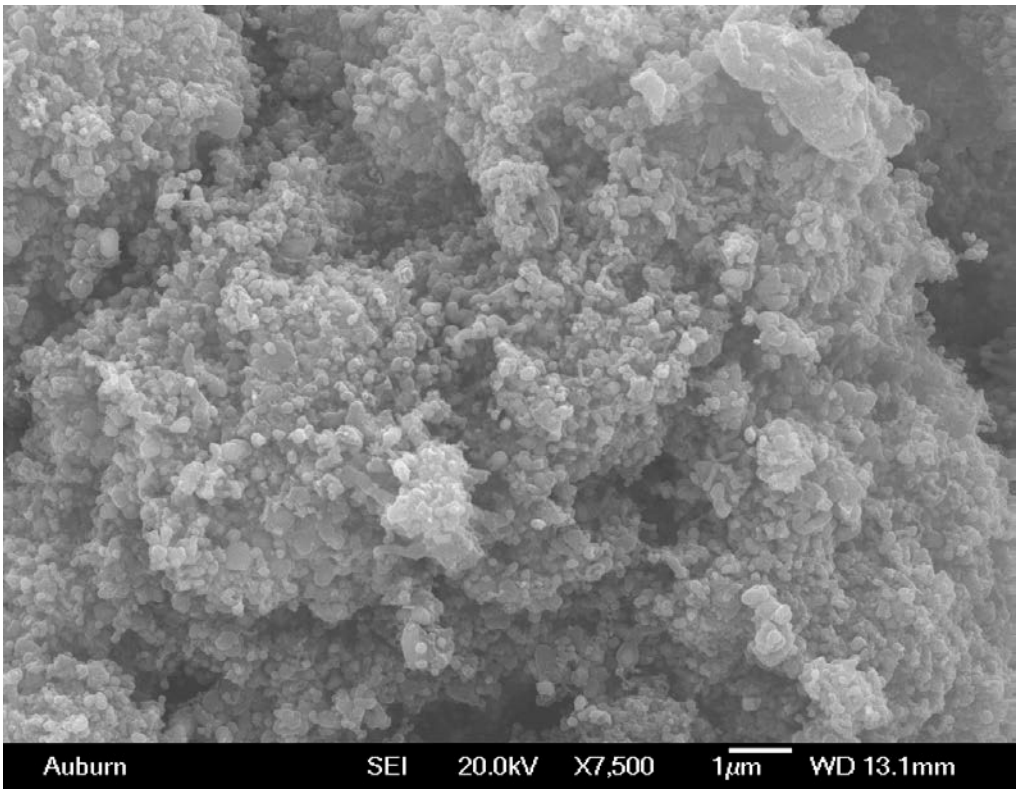


Figure 21 SEM images of MnO2/CNT sample with 0.1M HCl

There is basically no CNT produced with 0.1M HCl as the solution because the conductivity of PPy could be too low to let the hybrid burn in microwave. And the fact is that basically no burning can be seen during the microwave, which is the reason for no growth of CNT. So we further increase the concentration to 0.2M so that the CNT can grow with a good burning condition. Here is the SEM image.

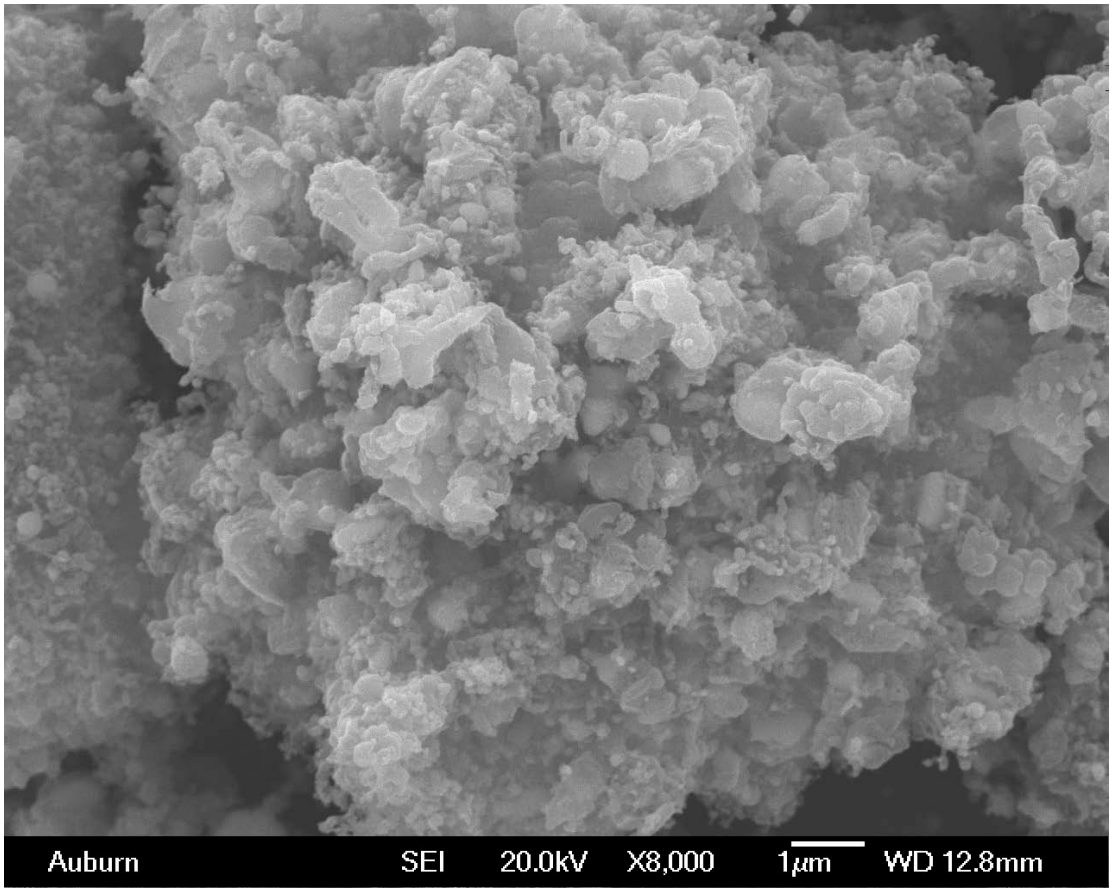


Figure 22 SEM images of MnO2/CNT sample with 0.2M HCl

Also, no CNT can be found which means HCl is still not enough to dope the PPy. So the concentration is increased to 0.5M.

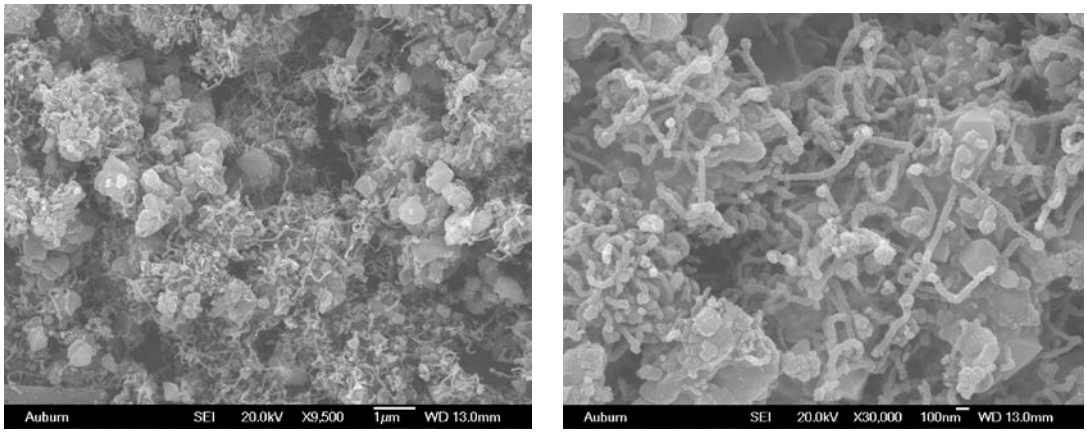


Figure 23 SEM images of MnO2/CNT sample with 0.5M HCl

A large and dense amount of flexible CNT along with $MnO_2$ can be seen all around the SEM images shown in figure 23, which is even better than the optimal condition (MnO2/Py as 4:1 in 1M HCl solution). So we further determine the final optimal reaction condition of this project, that is, 2g of MnO2 reacted with 0.5mL pyrrole (4:1) in a solution of 0.5M HCl. Moreover, the MnO2/PPy and MnO2/CNT following this reaction condition will be used to test the electrochemical property shown in **3.1.4 CV Test**.

### 3.1.2 TGA Characterization Results

In order to quantify MnO2 and PPy content in each and every nanocomposite structure, thermal characterization was applied by using the TGA instrument in a way that was described earlier. Since we have several different mass ratio of MnO2 to pyrrole to synthesize MnO2/PPy hybrid, there should be differences from their TGA curves. As the increase of temperature, PPy will be gradually decomposed and finally only MnO2 left in furnace. So with the different amount of MnO2, there could be difference shown in TGA curves.

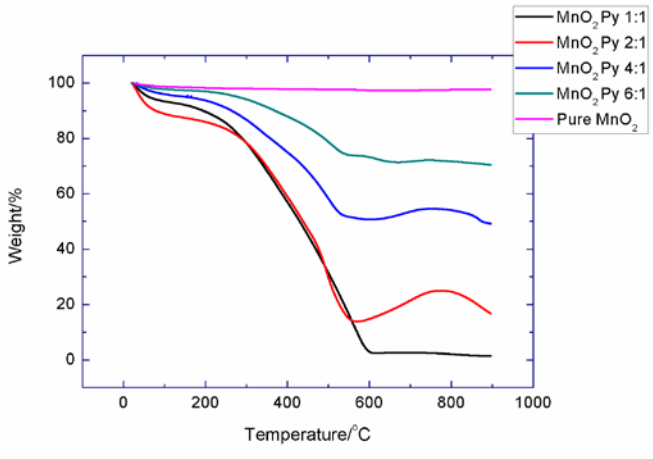


Figure 24 TGA graphics of MnO2/PPy hybrid with different ratio

| Ratio of MnO2 to Pyrrole | Practical weight left |
|---|---|
| 1 to 1 | 0% |
| 2 to 1 | 18.2% |
| 4 to 1 | 53.5% |
| 6 to 1 | 72.8% |

Table 3 Summary of TGA test results

The temperature is set, increasing from 20$^{o}$C to 900$^{o}$C with a rate of 10$^{o}$C/min. The circumstance in furnace is oxygen and a platinum pan is used to take the samples. Figure 23 showed the thermal analysis of MnO2/PPy hybrid with different MnO2/Py ratio. As the increasing amount of MnO2, we can find the plateaus are getting higher and higher, indicating more amount of MnO2 left in furnace. The controlled test is pure MnO2, which will prove that MnO2 will not decompose as temperature increase to 900$^{o}$C. When the ratio is 1 to 1, there is nothing left at 600 $^{o}$C. The reason is that the amount of MnO2 is so few that all of them have been lost in HCl solution. So there is only PPy left after synthesis and nothing left in TGA furnace. The loss of MnO2 not only happened in 1 to 1 case but also in the other several syntheses. Taking 6 to 1 as the example, the theoretical amount left in furnace might be 85.7%. But there are only less than 80% (around 75%) left, indicating the loss of MnO2 during the aqueous reaction. Table 3 has summarized the theoretical and practical weight left after TGA test to prove the loss of MnO2 during aqueous reaction. And we can also find a phenomenon that the less MnO2 used in reaction, the more MnO2 lost during the reaction.

The above TGA curve showed the thermal property of the hybrid with 1M HCl as the solution. Here we assumed that as the decrease of HCl concentration, the loss of MnO2 can

also be decreased. So we compare the TGA curve of MnO2/PPy hybrid with same ratio but different HCl concentration to prove our assumption.

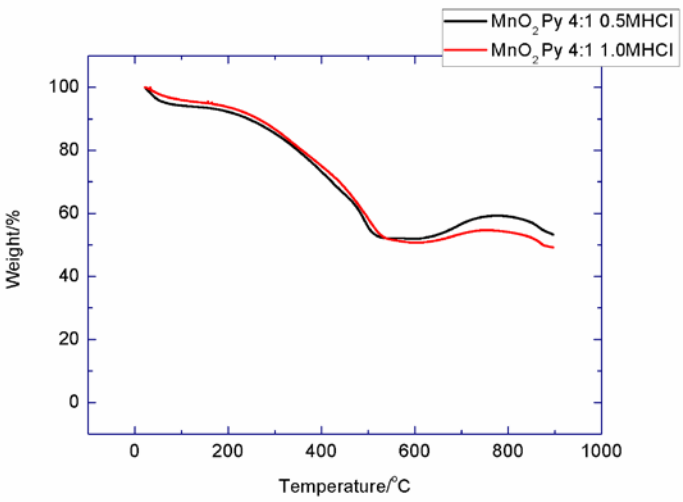


Figure 25 Comparative TGA graphics of MnO2/PPy hybrid with different HCl concentration

Figure 24 can prove our assumption. The concentration of HCl can affect the loss of $MnO_2$. With a more diluted HCl (0.5M), the amount of $MnO_2$ left is increased as shown in figure 24. Here in the curve we can also find the mass increase around 620$^{o}$C. This phenomenon can be attributed to the further oxidation of MnO2 because of the oxygen environment in the furnace. By absorbing oxygen, manganese can convert into a higher valence state such as +5 ($Mn_2O_5$) or +7 ($Mn_2O_7$).

### 3.1.3 FT-IR Characterization Results

To prove the success of oxidative polymerization of pyrrole within MnO2/PPy hybrid, FT-IR spectroscopy characterizations were applied to reseach the functional group in this hybrid and prove the precense of PPy.

As the comparison, we also test the IR of pure PPy as control to compare with our $MnO_2$/PPy composite.

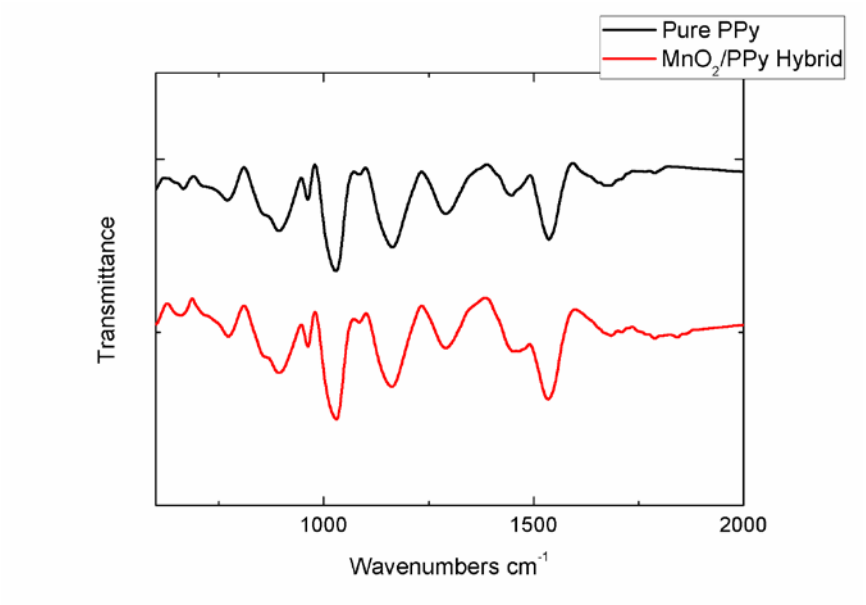


Figure 26 FT-IR spectra of Pure PPy and $MnO_2$/PPy hybrid

Very similar results, with some slight shiftings and intensity differences in peaks, were obtained from the FT-IR characterizations of these two metrials.

According to the FT-IR spectrum of pure PPy [24], several well-known PPy peaks were clearly observed at the corresponding wave numbers of 2733.3$cm^{-1}$ (C-H stretching vibrations), 1540.1$cm^{-1}$ (C-C and C=C stretching vibrations), 1446.1$cm^{-1}$ (C-N stretching), 1294.9$cm^{-1}$, 1160 $cm^{-1}$, and 1021.1$cm^{-1}$ (C-H and C-H in plane deformation modes) and finally 878.1$cm^{-1}$, 771.9$cm^{-1}$ and 657.4$cm^{-1}$ (C-H outer bending vibrations).

The hybrid sample was exhibiting very similar FT-IR peaks in its spectrum, by slightly shifting towards shorter wavelengths, at corresponding wave numbers of 2708.7$cm^{-1}$ (C-H stretching vibrations), 1536$cm^{-1}$ (C-C and C=C stretching vibrations), 1446.1 (C-N stretching), 1290.8$cm^{-1}$, 1156$cm^{-1}$, and 1012.9$cm^{-1}$ (C-H and C-H in-plane deformation modes) and finally 882.2$cm^{-1}$ and 706.5$cm^{-1}$ (C-H outer bending vibrations).

In summary, the FT-IR characterization of MnO2/PPy composite proves the PPy granule's presence in composite. The slight shiftings and intensity differences in peaks of such structure can be attributed to the interactions between PPy and MnO2.

### 3.1.4 Cyclic Voltammetry (CV) Application Results of Different Composites

Three different structures (Raw MnO2, MnO2/PPy and MnO2/CNT) were utilized to conduct electrochemical cyclic voltammetry (CV) applications by using Arbin-010 MITS Pro 4-BT 2000 instrument at standard laboratory conditions upon applying a sweeping potential from 0V to 1.0V at 20mV/s range. Ag/AgCl in a saturated solution of potassium chloride is used as the reference electrode. A pure platinum wire was used as the counter electrode and a purified graphite rods with above mentioned structures pasted at their tips by colloidal carbon, were used as the working electrodes. 50mL of 1M KCl aqueous solution was used as the electrolyte for these applications.

The purpose of this application was to obtain certain information about the electrochemical behavior of different as-prepared composite and to verify their applicability in supercapacitor via detecting the shape and area of the curves in their test results. Cyclic voltammograms (CVs) of each sample and related discussions were listed along the following paragraphs.

Here we mainly compare the CV curve of raw MnO2, MnO2/PPy and MnO2/CNT with the best nano--morphology. The aim is to obtain an enhancement of capacitive property from MnO2 based composite comparing to the raw stuff.

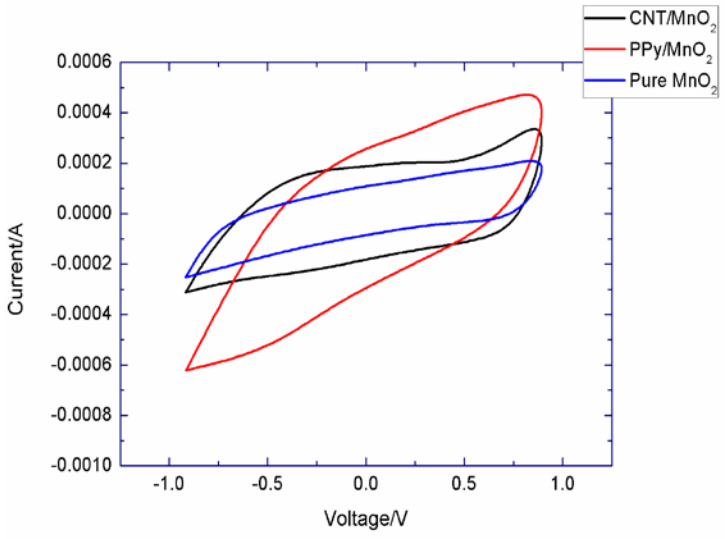

Figure 27 CV curves of raw MnO2, MnO2/PPy and MnO2/CNT

There are totally two key factors in CV to judge the capacitive property. The first one is the area of CV curve. A larger area indicates a higher value of capacitance. According to the definition of capacitance (C), C=(dI/dU)T where I is current, U is potential and T is time, here the integration of I to U is just the area of a current to voltage curve. So a CV curve is very proper to immediately and qualitatively judge the capacitive property of a material.

The second factor is the shape of CV curve[22]. As a capacitor, there shall be no unnecessary redox reaction during it charge and discharge electron. $MnO_2$ as a surpercapacitor will convert its valence between +4 and +3.

$$MnO_2(S) + 4H^+ + e^- \Longleftrightarrow Mn^{3+} + 2H_2O$$

There is only one electron's gain and loss. So the CV curve of MnO2 based capacitor could be very smooth and stable like a rectangular.

From figure 26, the pure $MnO_2$ (blue line) showed a very ideal rectangular shape as a capacitor. However, as I have mentioned in the very beginning of thesis, low conductivity will limit $MnO_2$'s capacitance. So the area of pure $MnO_2$ is very small comparing to MnO2/conducting materials composite, indicating a small value of capacitance.

For MnO2/PPy and MnO2/CNT composites, both of them have a relatively large curve area indicating a large value of capacitance. However, the shape of MnO2/PPy curve is very unstable and leaning, showing that besides the convert of Mn valence state, there are much more unnecessary redox reactions which are attributed to PPy happens. In comparison, there is only MnO2/CNT sample that showed both large curve area and a rectangular curve shape. The reason for it might be the stable and conductive nature of carbon nanotube.

In summary, MnO2/CNT is the best and ideal material in these three kinds of samples to serve as a surpercapacitor. And the assumption that enhancement of capacitive property from $MnO_2$ based composite comparing to the raw $MnO_2$ can be proved.

### 3.2 Characterizations for Microwaved $MnO_2$ based nanocomposite

#### 3.2.1 EDX Characterization Results

In this project, we use Mn(NO3)2 as the precursor to produce MnO2 in microwave. So the first thing needs to be done is to prove that the black powder after microwave is MnO2. Here we use elemental analysis to test what the sample is.

| Element | Weight/% | Atomic/% |
|---|---|---|
| O | 17.15 | 48.20 |
| Cl | 13.26 | 16.81 |
| Mn | 33.37 | 25.49 |
| Au | 36.23 | 9.50 |
| Totals | 100.00 | |

Table 4 Summary of the EDX analysis results of as-produced $MnO_2$

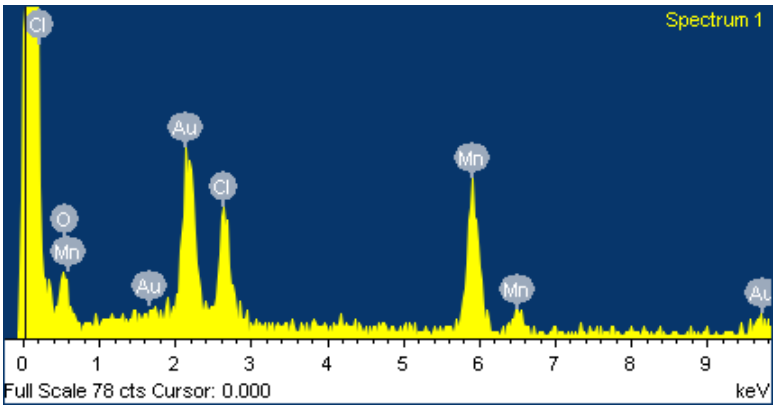


Figure 28 EDX analysis results of as-produced $MnO_2$

In table 3, we can find the element component of the sample which has oxygen of 48.20% and manganese of 25.49%. So the ratio of Mn to O is very close to 1:2, indicating

the main chemical formula of the sample is $MnO_2$.

### 3.2.2 SEM Characterization Results

Different morphology of manganese oxide composite structures were initially characterized by SEM to verify and prove the success of above mentioned synthesis methods. We first test the micromorphology of as-produced MnO2 as a controlled sample. The purpose for it is to rule out the possibility that MnO2 itself could make a contribution to a nanostructure.

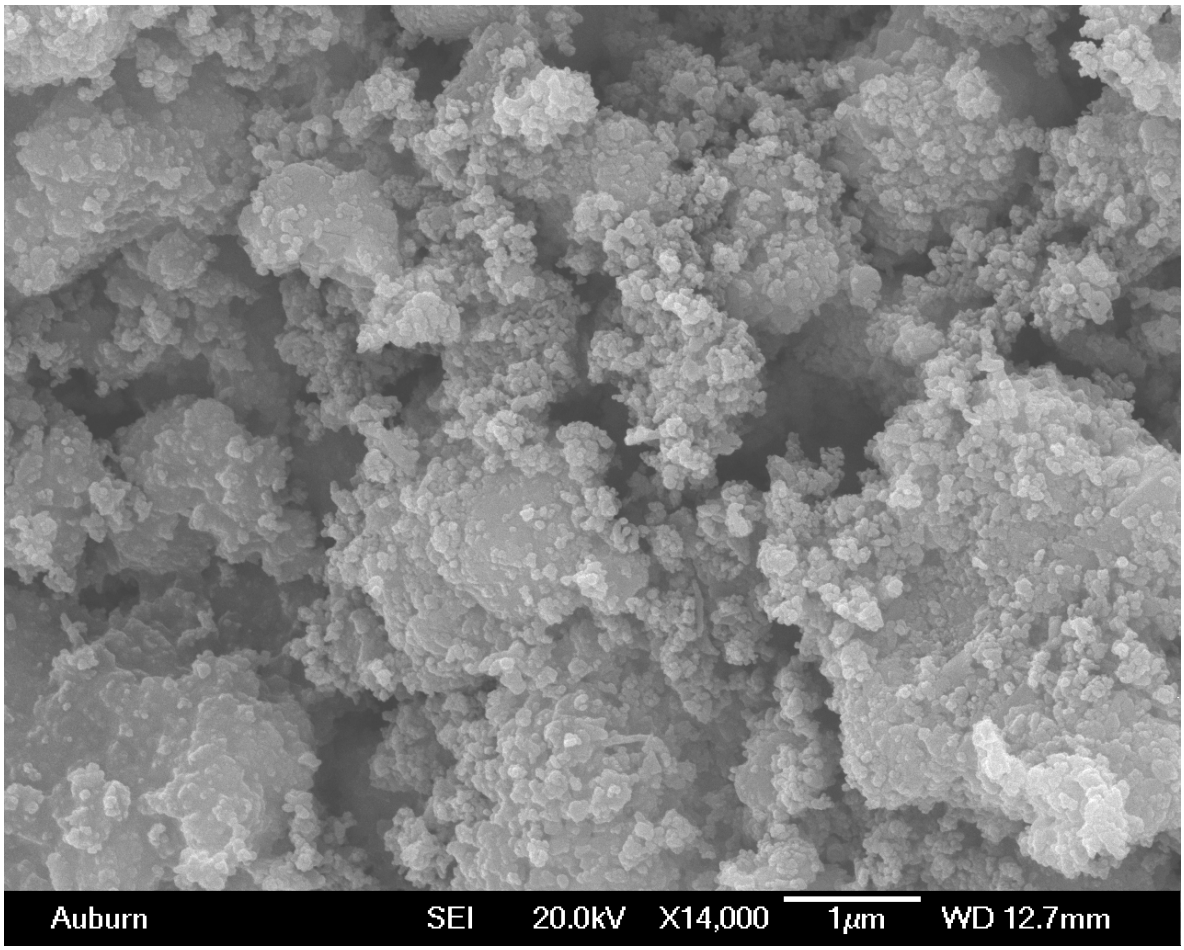


Figure 29 SEM image of as-produced MnO2

The SEM image above has shown an amorphous microstructure of the pure MnO2. There is no nanostructure but granule. So the possibility that pure MnO2 make a contribution to nanostructure can be ruled out.

The only difference on synthesis of this project from the last one is the choice of raw stuff (Mn(NO3)2 and commercial MnO2). And the following synthesis steps are basically the same because an optimal reaction condition had been determined, that is, 2g of MnO2 reacted with 0.5mL pyrrole (4:1) in a solution of 0.5M HCl. The same procedure also included the microwave step that 70mg of the as-synthesized hybrid blended with ferrocene by a mass ratio of 1 to 1 and heating in microwave.

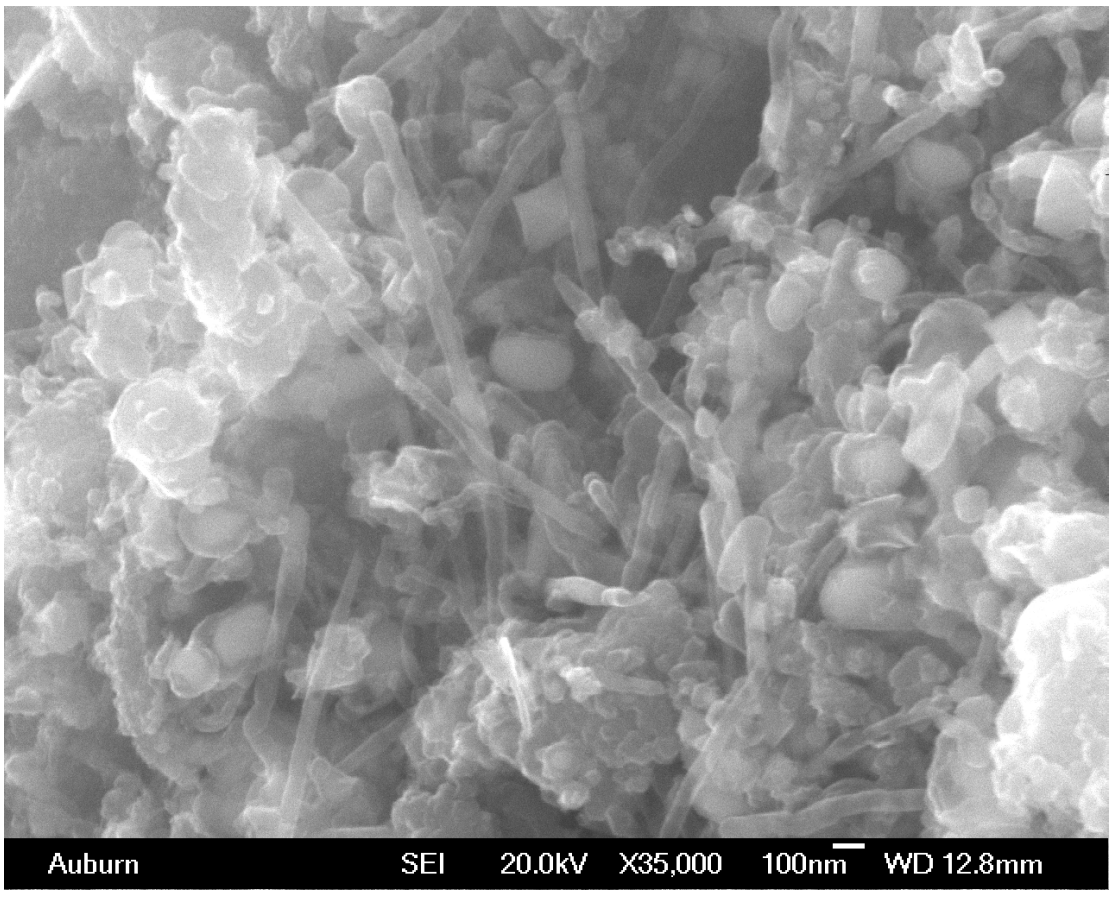


Figure 30 SEM image of MnO2/CNT nanocomposite after microwave

In the above SEM image we can find some tubelike nanostructures with a diameter below 100nm which are typical CNTs among the MnO2 granule. So we have verified and proved the success of aqueous--phase synthesis method. And this MnO2/CNT nanocomposite along with MnO2/PPy hybrid following the as mentioned optimal reaction condition will be used to test the electrochemical property later.

### 3.2.3 FT-IR Characterization Results

In order to prove the success of oxidative polymerization of pyrrole within MnO2/PPy hybrid, FT-IR spectroscopy characterizations were applied to test the functional group in this hybrid and prove the precense of PPy. We also test the IR of pure PPy as control to compare with $MnO_2$/PPy composite.

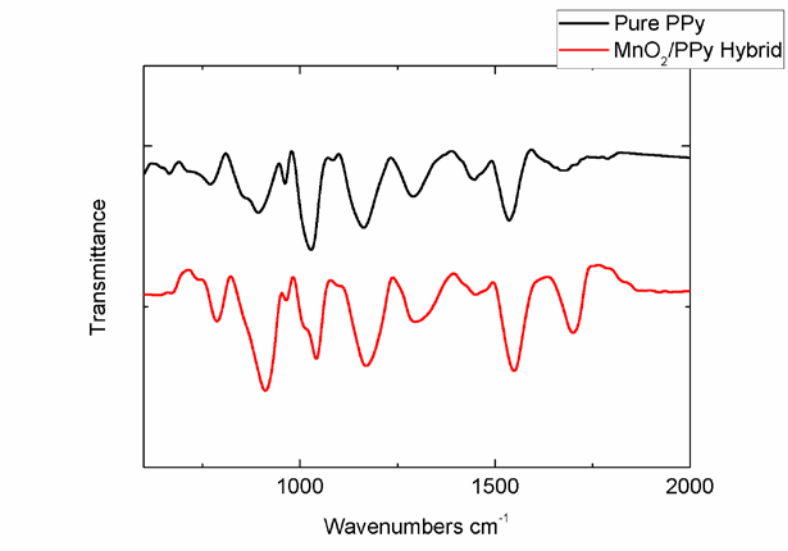


Figure 31 FT-IR spectra of Pure PPy and $MnO_2$/PPy hybrid

Very similar results, with some slight shiftings and intensity differences in peaks, were obtained from the FT-IR characterizations of these two metrials.

According to the FT-IR spectrum of pure PPy [24], several well-known PPy peaks were clearly observed at the corresponding wave numbers of 2733.3$cm^{-1}$ (C-H stretching vibrations), 1540.1$cm^{-1}$ (C-C and C=C stretching vibrations), 1446.1$cm^{-1}$ (C-N stretching), 1294.9$cm^{-1}$, 1160 $cm^{-1}$, and 1021.1$cm^{-1}$ (C-H and C-H in plane deformation modes) and finally 878.1$cm^{-1}$, 771.9$cm^{-1}$ and 657.4$cm^{-1}$ (C-H outer bending vibrations).

The hybrid sample was exhibiting very similar FT-IR peaks in its spectrum, by slightly shifting, at corresponding wave numbers of 2708.7$cm^{-1}$ (C-H stretching vibrations), 1524$cm^{-1}$ (C-C and C=C stretching vibrations), 1446.1 (C-N stretching), 1286.7$cm^{-1}$, 1151$cm^{-1}$, and 1022.9$cm^{-1}$ (C-H and C-H in-plane deformation modes) and finally 872.2$cm^{-1}$, 763.2$cm^{-1}$ and 674.5$cm^{-1}$ (C-H outer bending vibrations).

So the FT-IR characterization of MnO2/PPy composite proves the PPy granule's presence in composite. The slight shiftings and intensity differences in peaks of such structure can be attributed to the interactions between PPy and MnO2.

### 3.2.4 TGA Characterization Results

TGA is used to quantify MnO2 and PPy content in composite. Here since we have adapted the optimal reaction condition, there is only one sample tested and compared with as-produced raw MnO2. We set the temperature increasing from 20$^{o}$C to 900$^{o}$C with a rate of 10$^{o}$C/min. The circumstance in furnace is oxygen and a platinum pan is used to contain the samples.

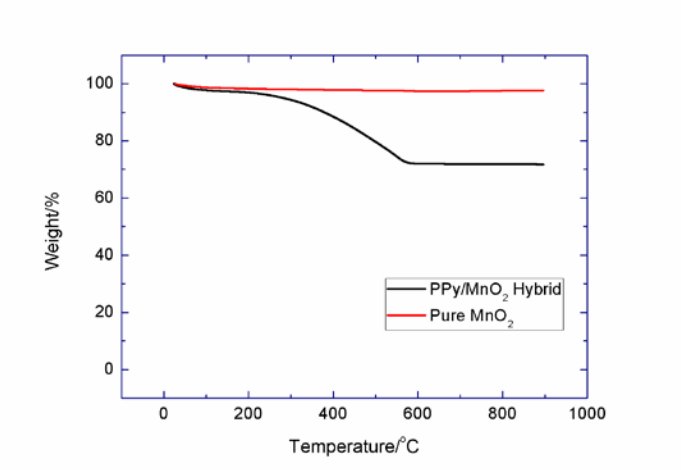


Figure 32 Comparative TGA graphics of MnO2/PPy hybrid with raw MnO2

From figure 32 we can find that PPy granule will start to decompose at around 250 $^{o}$C. All of the PPy component will be burned out at around 600 $^{o}$C to from a plateau and the left material is MnO2. The mass ratio of MnO2 to PPy is 4:1. Thus, theoratically the amount left after heating is 80%. However, the practical value is less than 70%, again indicating the loss of MnO2 during the aqueous reaction in an acidic condition. And this problem can be solved by a solid—phase reaction which will be mentioned in detail at part 3.3.

### 3.2.5 Cyclic Voltammetry (CV) Application Results of the Composites

Three different structures (Raw MnO2, MnO2/PPy and MnO2/CNT) were utilized to conduct electrochemical cyclic voltammetry (CV) applications by using Arbin-010 MITS Pro 4-BT 2000 instrument at standard laboratory conditions upon applying a sweeping potential from 0V to 1.0V at 20mV/s range. All the electrodes and electrolyte are the same as what have been described earlier. Here we mainly compare the CV curves of raw MnO2, MnO2/PPy and MnO2/CNT with the best nano--morphology. The aim is to obtain an

enhancement of capacitive property from MnO2 based composite comparing to the raw sample.

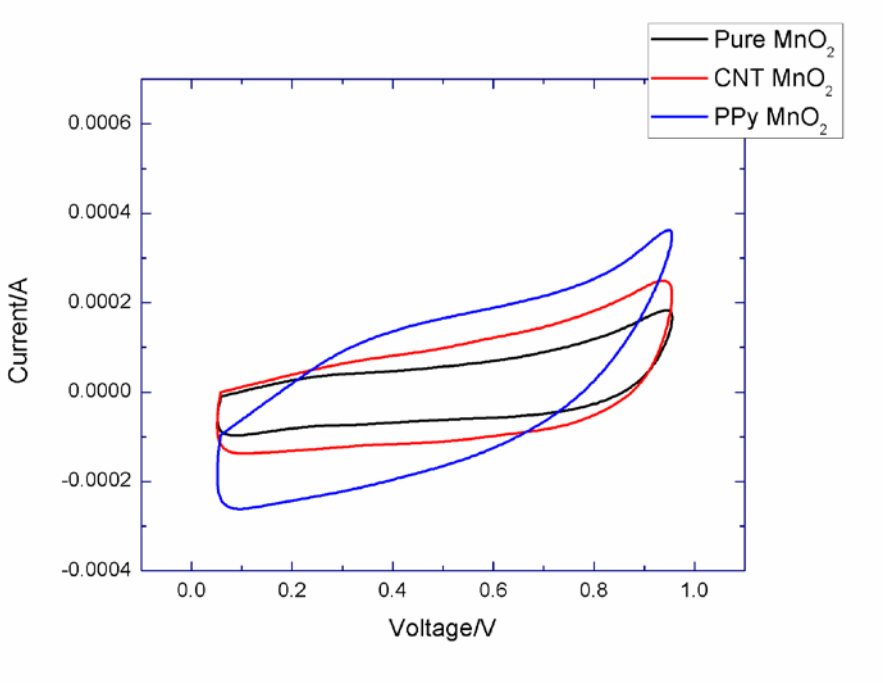


Figure 33 CV curves of raw MnO2, MnO2/PPy and MnO2/CNT in 1M KCl at 20mV/S

As described earlier. Two main factors determine the capacitive property in CV are the shape and area of curve. Still pure MnO2 has shown a stable curve shape but the low area represent a relatively low capacitance. And PP/MnO2 hybrid showed a promising value of capacitance due to a large curve area. However, the unstable curve shape has proved that some redox reactions from PPy happened, which will impact the normal work of capacitor. We can clearly find a oxidative peak of PPy at around 0.4V which will disturb the charge—discharge from manganese. So in comparison, CNT/MnO2 nanocomposite possessed both a obviously larger curve area and a very stable curve shape, indicating a promising capacitive property.

### 3.2.6 Charge—discharge Test Results of the Composites

Charge/discharge test is another general electrochemical test to research the capacitive property of materials. In this method, by setting a certain potential drop and current density, electrons will be charged and discharged cycle by cycle within a range of as set potential. Researchers need to record the time consumed to discharge the electrons from a maximum potential to minimum. The specific capacitance of the electrode at different current density is calculated by C= it/mV from the discharge curves, where i is the constant discharge current, m is the mass of the samples in the electrode ( i/m is current density), t is the discharge time, and V is the potential drop during discharge. In our research, the potential drop is from 1.0V to 0V and the current density is 1A/g.

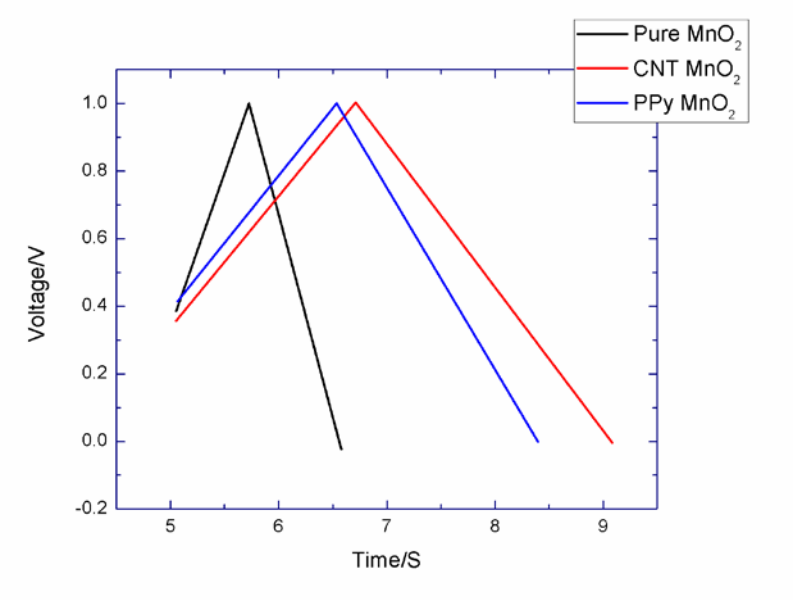


Figure 34 Discharge curves of raw MnO2, MnO2/PPy and MnO2/CNT in 1M KCl at current density of 1A/g

From the above testing curves we can find that CNT/MnO2 has the longest discharge time comparing to the other two samples, according to the equation of capacitance described earlier, which means the specific capacitance of CNT/MnO2 is the highest

among the three tested samples.

### 3.3 Characterizations for solid-phase $MnO_2$ based nanocomposite

This is a method designed in order to avoid the loss of MnO2 during the aqueous phase reaction in an acidic condition. As I have described earlier in synthesis methods part, Mn(NO3)2 will immediately blend with PPy nanofiber and then microwave the mixer to form a MnO2/PPy hybrid. Below are the characterizations for the product made from this method.

#### 3.3.1 SEM Characterization Results

We totally have 3 controlled experiments in this project in order to determine the optimal ratio of PPy to Mn(NO3)2. And the morphology of MnO2/PPy obtained after microwave is standard to judge the ideal ratio of PPy and Mn(NO3)2. The 3 different ratios are 3:1, 2:1 and 1:1 (PPy to Mn(NO3)2). Here are the SEM images of as-produced PPy/MnO2.

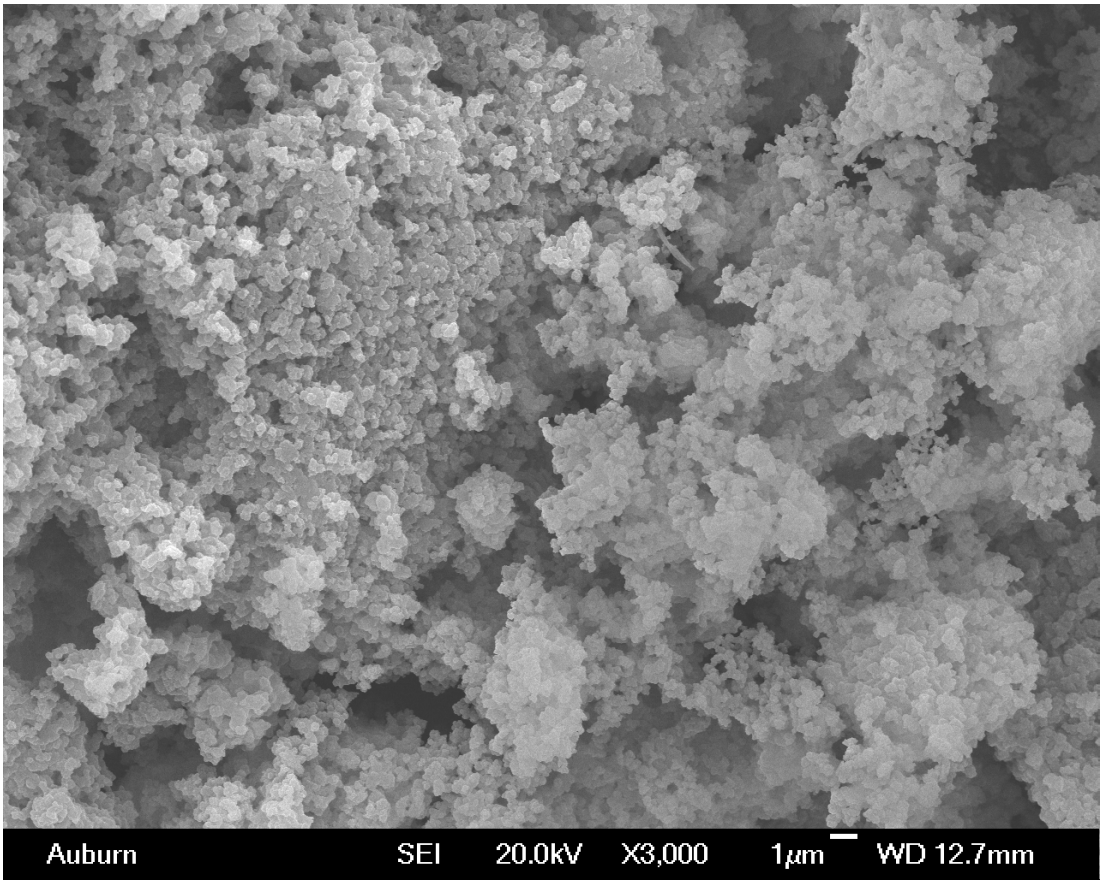

Figure 35 SEM image of PPy/MnO2 with a ratio of PPy to Mn(NO3)2 is 1:1

In the above SEM image we can not find the PPy nanofiber because the amount of Mn(NO3)2 is so large that all of the as-produced MnO2 covering on PPy nanostructure. So the amount of manganese compound needed to be reduced.

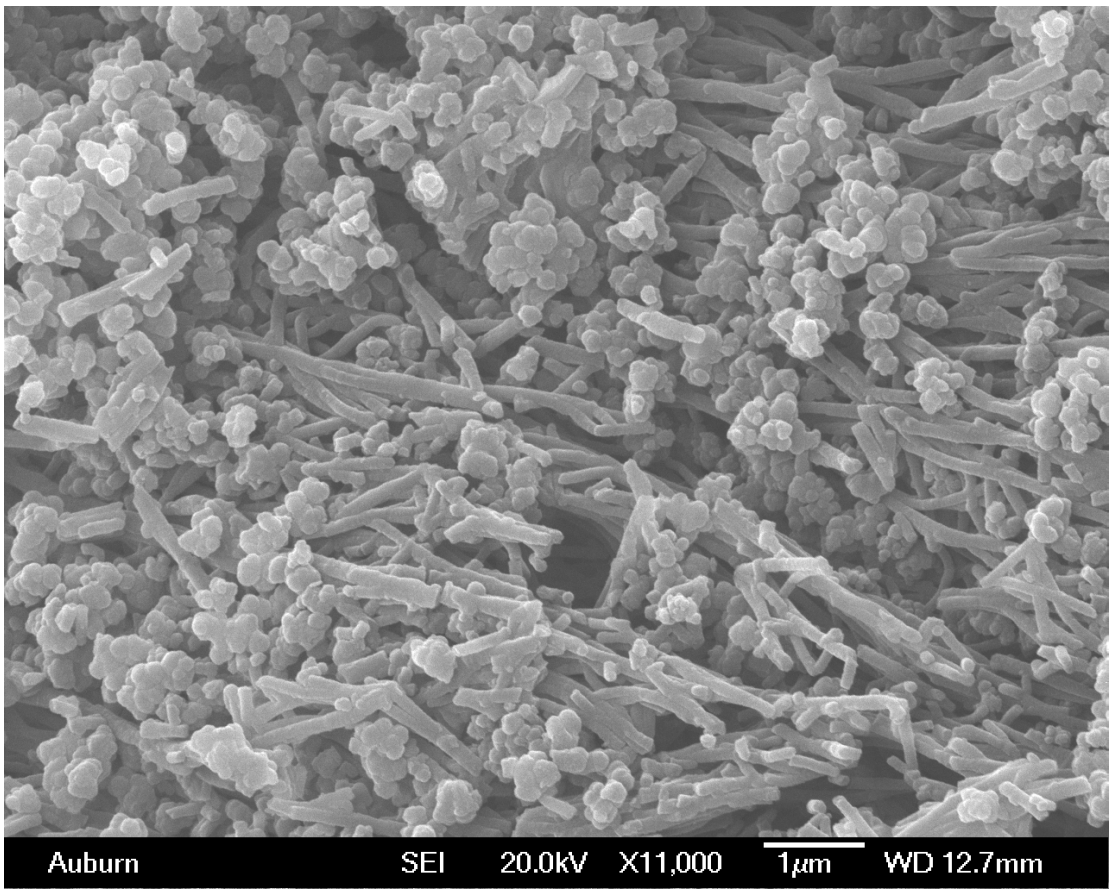


Figure 36 SEM image of PPy/MnO2 with a ratio of PPy to $Mn(NO_3)_2$ 2:1

At ratio of 2:1, we can find that as-produced MnO2 particles are uniformly dispersed among the PPy nanofiber. And the most of the particles have a diameter below 500nm according to the scale bar. So at this ratio, the morphology of MnO2/PPy hybrid is relatively uniform. In order to test if the 2:1 is the optimal ratio, we further increase the ratio to 3:1.

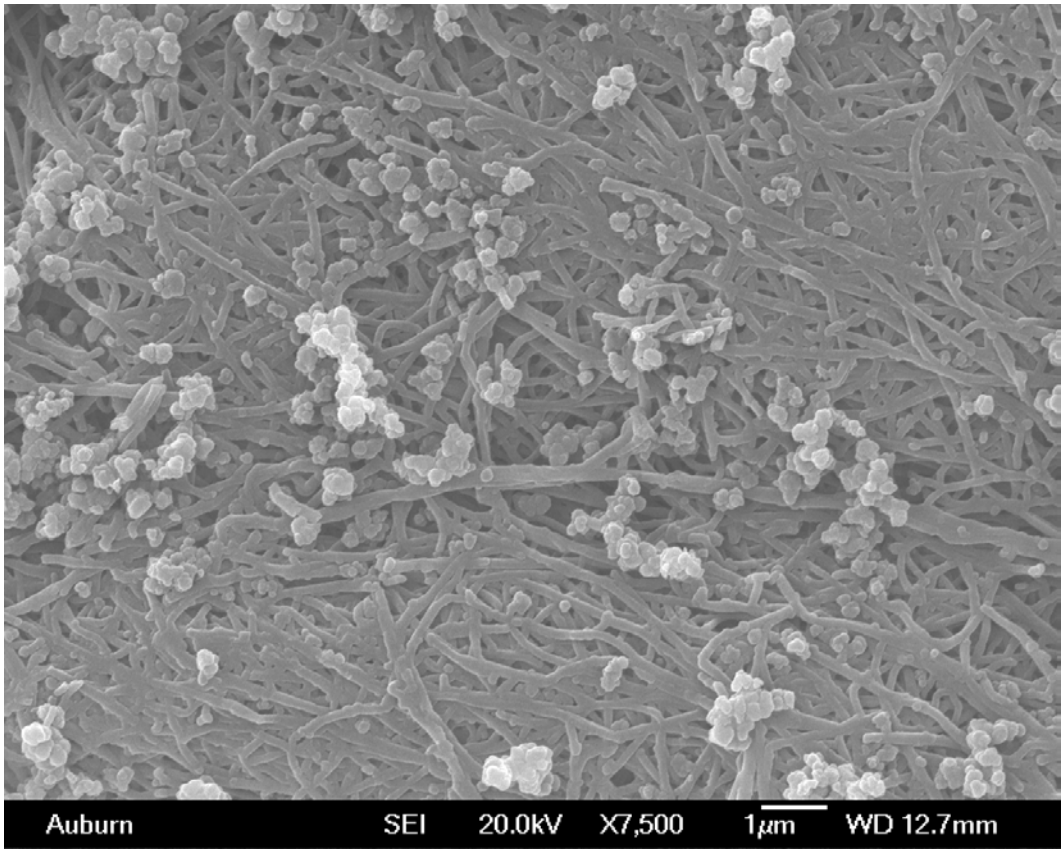


Figure 37 SEM image of PPy/MnO2 with a ratio of PPy to $Mn(NO_3)_2$ 3:1

The amount of MnO2 disperses among PPy fiber is very few comparing to the ratio of 2:1. And most of the MnO2 granule aggregate together with a diameter beyond 1um. Since MnO2 is the major capacitive part, the electrochemical property can not be promised in this case. The MnO2 particle in the material is so few but still aggregate to form a large bulk, which is not preferred as a good dispersion condition. Thus, we determine the PPy to $Mn(NO_3)_2$ ratio 2:1 as the optimal reaction condition. And the as produced sample is further microwaved with ferrocene following the method described earlier to obtain the CNT/MnO2 nanocomposite.

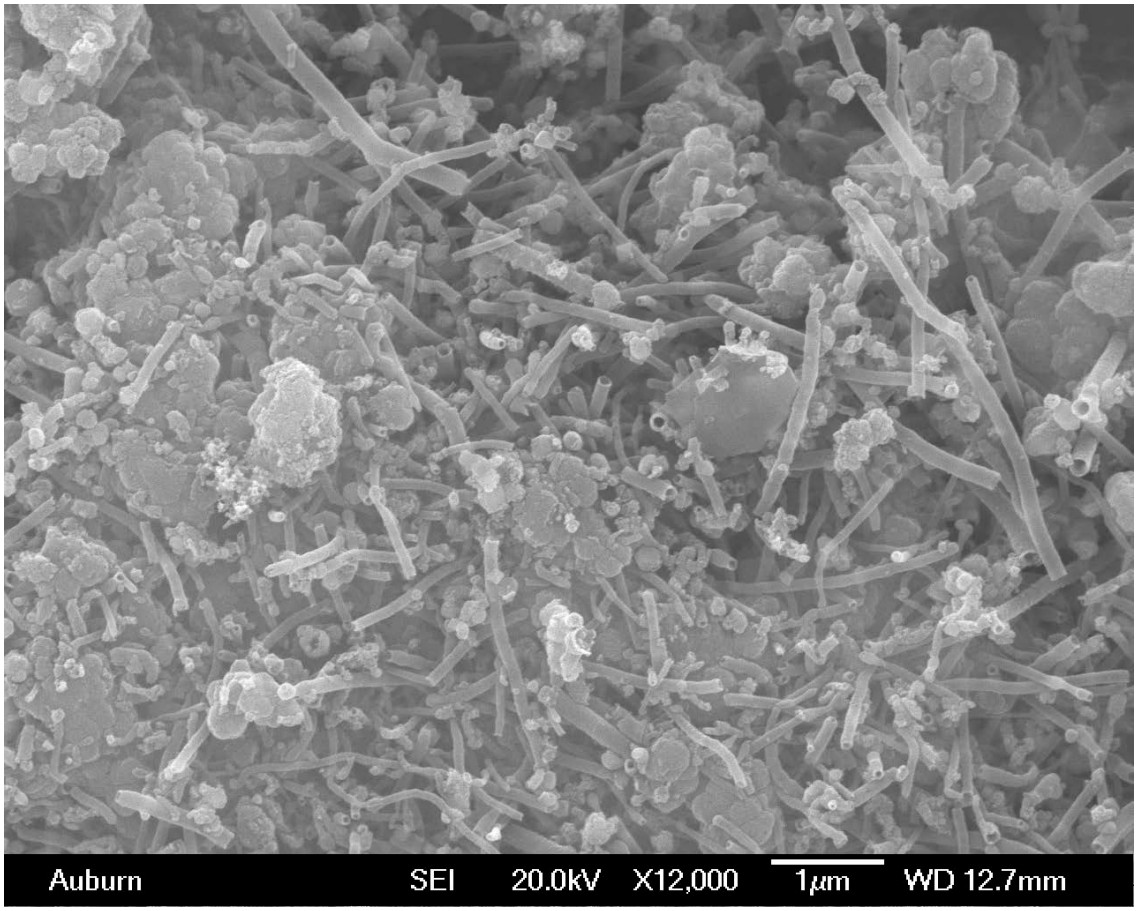


Figure 38 SEM image of MnO2/CNT nanocomposite after microwave

You may think the nanostructures shown in the above SEM image are PPy nanofibers which have been present in the composite. But it is not difficult to tell the nanotube structures with a hollow core which is the typical structure for CNT. And the diameter of CNT produced is around 150nm. The granular structure among CNT is MnO2. So the SEM test can successfully prove that CNT can grow under the microwave condition from a mixer of MnO2/PPy and ferrocene.

### 3.3.2 TGA Characterization Results

Since we have 3 different ratios as the controlled experiments, it is necessary to further quantitatively determine the amount of MnO2 among the PPy/MnO2 hybrid. Please note that these 3 different ratios are PPy to Mn(NO3)2 but not pure MnO2. So we need to

one step of further calculation according to the chemical formula of Mn(NO3)2 decompose.

According to the chemistry reaction formula of Mn(NO3)2, after full burning, the sample left could be 48.6% approaching to 50% and the rest is $N_2O_4$ gas out of the system. So if the ratio of PPy to $Mn(NO_3)_2$ is 1:1, after microwave, the ratio of PPy to MnO2 can reach to 2:1. So the theoretical weight left after TGA test should be 1/3, that is, 33.3%.

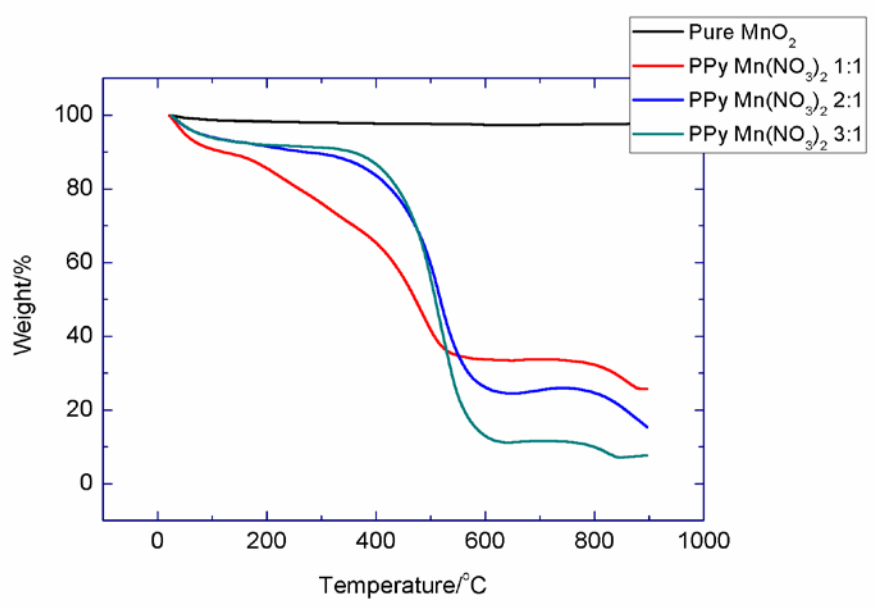


Figure 39 Comparative TGA graphics of MnO2/PPy hybrid with different ratio of PPy to $Mn(NO_3)_2$

Here is the table that summarized the theoratical and practical weight left in TGA test.

| Ratio PPy to Mn(NO3)2 | Theoretical weight left | Practical weight left |
|---|---|---|
| 1 to 1 | 33.3% | 32.4% |
| 2 to 1 | 20.0% | 21.6% |
| 3 to 1 | 14.2% | 13.5% |

Table 5 Summary of TGA test results

In table 5 we clearly find that the practical weight left is very approached to the theoretical one, indicating that the loss of MnO2 can be avoided by using this so—called solid phase reaction just because no acidic solution will solve the MnO2 any more.

### 3.3.3 Cyclic Voltammetry (CV) Application Results of the Composites

The procedure of CV test is all the same as what the last two projects have done. And we just follow the two standards mentioned not only one time earlier to judge the capacitive property of tested samples.

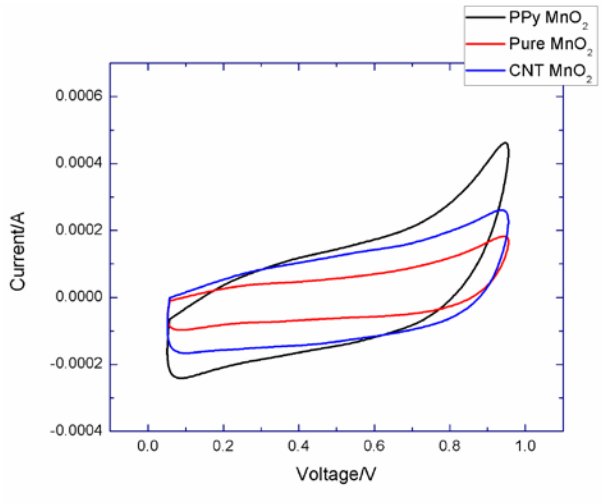


Figure 40 CV curves of raw MnO2, MnO2/PPy and MnO2/CNT in 1M KCl at 20mV/S

Very similar with the composite made by the last method, the stable but small curve area is the raw MnO2. Large curve area but an unstable curve shape is the PPy/MnO2 hybrid due to the additional redox reactions from PPy. Only MnO2/CNT nanocomposite made by microwave method can possess both stable curve shape (a typical rectangular shape) and a relatively large curve area.

In summary of the all these three project, they have the same trend, that is, the stable but low capacitance raw MnO2 can be enhanced by adding conducting polymer PPy but the problem is that the composite become unstable. Then by microwaving the sample with ferrocene to grow some CNTs in it, the final MnO2/CNT composite has been proved not only a large value of capacitive but also a very stable nature to serve as a supercapacitor.

### 3.3.4 Charge—discharge Test Results of the Composites

The specific capacitance of the electrode at different current density is calculated by C= it/mV from the discharge curves, where i is the constant discharge current, m is the mass of the samples in the electrode ( i/m is current density), t is the discharge time, and V is the potential drop during discharge. By setting a certain potential drop and current density, we recorded the time consumed to discharge. The longer of discharge time, the higher of capacitance.

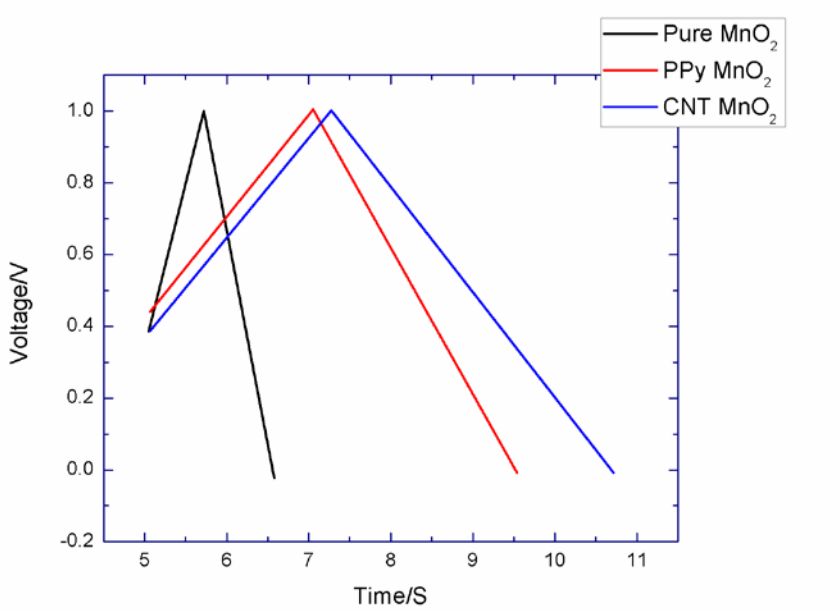


Figure 41 Discharge curves of raw MnO2, MnO2/PPy and MnO2/CNT in 1M KCl at current density of 1A/g

From the above testing curves we can find that CNT/MnO2 has the longest discharge time comparing to the other two samples, according to the equation of capacitance described earlier, which means the specific capacitance of CNT/MnO2 is the highest among the three tested samples. So the charge/discharge test can solve the problem of CV test because we can not tell which one has a larger curve area in CV curve. But from charge/discharge test we can use a quantitative equation to determine whose value of capacitance is larger. It was believed that this kind of MnO2/CNT nanocomposite structures would play an important role in the development of highly efficient, next-generation supercapacitor.

# CHAPTER 4

# CONCLUSIONS AND THE FUTURE WORK

## 4.1 Conclusions

This Master's thesis describes experimental details in investigating the electrochemical properties of MnO2 based nanocomposites, and confirming the potential applications as active components of supercapacitor.

In this study, a novel, fast chemical oxidative polymerization of pyrrole monomers can be adapted to react with manganese oxide. And this composite can further serve as the substrate for the fast growth (only 2 minutes) of carbon nanotube under the microwave condition with ferrocene as the precursor of carbon. So the whole experiments are very novel and time-saving.

The capacitive property of the as-synthesis MnO2 based nanocomposite have a dramatically enhancement comparing to pure MnO2, which has solved the problem rose at the very beginning of this thesis.

## 4.2 Future Work

In this research, we mainly focus on the modification of materials' morphologies, comparison of different materials' capacitive property and draw a qualitative conclusion. In future work, we will make much more efforts to get the quantitative statistic about how much the value of capacitance for MnO2 based nanocomposites has increased. And making sure our novel nanocomposites do have the potential to become the next generation of supercapacitor.

## References


1 J.P. Zheng, Electrochem. *Solid-State Lett*. 1999, **2**, 359

2 Fei Teng, Sunand Santhanagopalan, Dennis Desheng Meng *Solid State Sciences*. 2010, **12**, 1677-1682

3 http://en.wikipedia.org/wiki/Manganese_dioxide

4. Greenwood, Norman N.; Earnshaw, Alan. *Chemistry of the Elements*. 1984 Oxford: Pergamon Press. 1218–1220.

5. Preisler, Eberhard *Chemie in unserer Zeit.* 1980, **14**, 137–48,

6. Q. Feng, H. Kanoh and K. Ooi., *J. Mater. Chem.* 1999, **9**, 319.

7 A. R. Armstrong, H. Huang, R. A. Jennings and P. G. Bruce, *J. Mater. Chem.* 1998, **8**, 255.

8 Y. Chabre and J. Pannetier, *Prog. Solid St. Chem.* 1995, **23**, 1

9. O. Schilling and J. R. Dahn, *J. Appl. Cryst.*, 1998, **31**, 396

10. Xun Wang and Yadong Li *J. AM. CHEM. SOC***.** 2002, **124**, 2880

11 Thackeray, M. M. *Prog. Solid State Chem.* 1997, **25,** 1.

12 P. M. De Wolff, J. W. Visser, R. Giovanoli and R. Brutsch, *Chimia*, 1978, **32**, 257

13 Ramakrishnan, S. *Resonance* 1997, 48-58

14 Pratt, C. Essay on conducting polymers 1996, 1-7

15 Zhang, X. PFEN 7970 Conductive polymer materials - Lecture 2 **2010**, Auburn University, Auburn, Alabama

16 Jianfeng Zang and Xiaodong Li *J. Mater. Chem.,* 2011, **21**, 10965–10969

17 Jaidev, Razzak Imran Jafri, Ashish Kumar Mishra and Sundara Ramaprabhu *J. Mater. Chem.,* 2011, **21**, 17601–17605

18 Zhang, X.; Manohar, S. K. *Chem. Commun.* **2006**, 2477-2479

19 Lu, X.; Chao, D.; Chen, J.; Zhang, W.; Wei, Y. *Materials Letters,* 2006**, 60,** 2851-2854

20 http://metallome.blogspot.com/2009/03/drawing-ferrocene.html

21. Zhang, X. Synthesis of nanostructured polymers, Dissertation, **2005**, The University of Texas at Dallas, Dallas, Texas

22 Yaohui Wang, Hao Liu, Xueliang Sun and Igor Zhitomirsky *Scripta Materialia* 2009, **61**, 1079–1082

23 R.K. Sharma, A.C. Rastogi, S.B. Desu *Electrochimica Acta* 2008, **53**, 7690–7695

24 Selcuk Poyraz Synthesis and Characterization of Nanostructured Conducting Polymers and Their Composites with Noble Metal Nanoparticles , Master's thesis, **2010,** Auburn University

25 Adrian Porch, Daniel Slocombe and Peter P. Edwards *Phys. Chem. Chem. Phys.*, 2013,**15**, 2757-2763

26 Zhen Liu , Jialai Wang , Vinod Kushvaha , Selcuk Poyraz , Hareesh Tippur , Seongyong Park , Moon Kim , Yang Liu , Johannes Bar , Hang Chen and Xinyu Zhang *Chem. Commun.*, 2011,**47**, 9912-9914